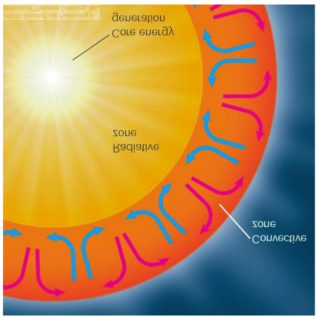

MSc

Structural changes in ionization regions inside sun-like stars

Liliana Novais,
Mestrado em Astronomia
Departamento de Física e de Astronomia

2017

Orientador
Ilidio P. Lopes,Professor Auxiliar com Agregacao, Instituto Superior Técnico

U.PORTO

FACULDADE DE CIÊNCIAS
UNIVERSIDADE DO PORTO

Todas as correções determinadas pelo júri, e só essas, foram efetuadas.

O Presidente do Júri,

Porto, / /

MSc

FACULDADE DE CIÊNCIAS DA UNIVERSIDADE DO PORTO

Structural changes in ionization regions inside sun-like stars

by

Liliana Novais

A thesis submitted in partial fulfillment for the degree of Masters on Astronomy

in the

Faculdade de Ciências da Universidade do Porto
Astronomy and Physics Department

January 2018

ISBN :9781370075973

Declaration of Authorship

I, Liliana Novais, declare that this thesis titled, 'Structural changes in ionization regions inside sun-like stars' and the work presented in it are my own. I confirm that:

- This work was done wholly or mainly while in candidature for a research degree at this University.
- Where any part of this thesis has previously been submitted for a degree or any other qualification at this University or any other institution, this has been clearly stated.
- Where I have consulted the published work of others, this is always clearly attributed.
- Where I have quoted from the work of others, the source is always given. With the exception of such quotations, this thesis is entirely my own work.
- I have acknowledged all main sources of help.
- Where the thesis is based on work done by myself jointly with others, I have made clear exactly what was done by others and what I have contributed myself.

Signed:

Date:

This page was left Blank

"Man must rise above the Earth—to the top of the atmosphere and beyond—for only thus will he fully understand the world in which he lives."

- Socrates, Philosopher

This page was left Blank

Acknowledgements

First of all, I want to thank my family for all the support that they gave me for this last two years, specially their patience and their enthusiasm everytime I talked about my thesis, results and problems. For earing me when I got frustratd with the results and happy when I got pass an obstacle. Specially for my young daughter Isabel, for understanding that sometimes I could not play because I was working and her support and interest in knowing more about my work.

I cannot forget my advisor, Ilídio Lopes, for his help and for believing in me when I first contacted him to be my supervisor in this thesis. For his support that helped me evolve as a researcher and to learn a subject that fashinated me for a long time.

I want to thank the CAUP for allowing me to use one of they offices. Specially, João Lima, and Pedro Viana, for all their help.

I also want to thank Benard Nsamba for helping me in some question on MESA and on asteroseismology, and his patience for all my doughts.

And finally all the MESA community for helping me and for developing the program, that helped to build the models for my thesis.

FACULDADE DE CIÊNCIAS DA UNIVERSIDADE DO PORTO

Abstract

Faculdade de Ciências da Universidade do Porto

Astronomy and Physics Department

Masters on Astronomy

by Liliana Novais

Understanding the origin of the magnetic field in the upper layers of the Sun and sun-like stars is one of most important problems of current stellar astrophysics. In this study, we investigated how the microscopic structure of the envelope of sun-like stars could create or suppress the magnetic fields observed in the surface in some low-mass stars. In particular, we analysed how the ionization levels of different chemical elements in stellar models with or without differential rotation could affect the magnetic activity of stars.

In order to do so, we used the Modules for Experiments in Stellar Astrophysics (MESA), to compute 1D models for four stars, HD 10700 (Model A), HD 1835 (Model B), HD 190360 (Model C) and the Sun (Model D) which are known to have different degrees of magnetic activity. The observational evidence of magnetic activity on these stars is discussed in the Baliunas et al paper [1995].

The goal of this project was to find out how the evolution of the star alter the inner structure of the stellar envelope, and how in turns this affects the ionization levels of different chemical elements (Hidrogen, ^{1}H, Helium, ^{4}He, Carbon, ^{6}C, Oxygen, ^{8}O, Nitrogen, ^{7}N, Neon, ^{10}Ne, Silicium, ^{14}Si, Magnesium, ^{12}Mg, and Iron, ^{26}Fe) and the radial distribution of mean free electrons per nucleon, and from that we infer possible links to the magnetic activity of the star.

The Sun (Model D) and HD 10700 (Model A) were used as references to test the quality of our stellar models, since these are the best-known stars in this study. The first because it is the most well-known and studied star that establish the standard physics use in the modelling of main-sequence stars of low-mass, and the second star was chosen since this one was targeted for an astereoseismological study by Teixeira et al [2009], and therefore some observational data is available.

We found that the evolution with and without rotation causes important structural changes in the stars, mainly in the location and size of the convective zone, affecting the distribution of the ionization states of the chemical elements for the four stars. Equally, the distribution of mean free electrons per nucleon changes significantly in the models build for the stars under study, these differences may influence the evolution of a magnetic cycle. The star HD 10700 seems to present the larger differences on this quantity, with a variation up to 8%. These changes on the distribution of charges inside the star, may be responsible by significant differences in the formation and maintenance of the magnetic cycles among stars, resulting in quite distinct magnetic cycles.

Accordingly, HD 1835 (Model B) is the star that present the strong magnetic activity that has a mean free electron per nucleon in the core 20% above the value found for the Sun(Model D). HD 10700 (Model A)that is known to not have a significant magnetic activity presents a value of 10% lower than the Sun (Model D). Finally, HD 19360 (Model C) seems that it does not present any magnetic activity, but presents the number of mean free electron per nucleon identical to the Sun (Model D), being the star that presents the closest distribution of all studied quantities closer to the solar case, represented by Model D.

Moreover, we have also present some asteroseismology results. HD 10700 (Model A) presents almost no modulation in all computed astereoseismic quantities: large separation, small separation and second difference. In the case of the other three stars, it is possible to identify a seismic signature related with the presence of differential rotation. HD 190360 (Model C) and HD 1835 (Model B) are high metallicity stars with different ages, the profiles are similar but the values for all computed quantities are quite different. This could be a clear evidence of age and a result of evolution, or a evidence of their magnetic inactivity that makes their profiles closer to the solar case.

All stars present in this study show different internal structures that changed significantly when rotation is implemented, as mentioned before the most affected region is the

convection zone. These changes seem to be strong depending on the age and metallicity of each model. Stars with a lower metallicity seem to be more influenced by this effect than stars with an higher metallicity.

Keywords: solar-like stars, internal structure, evolution, rotation, asteroseismology, ionization levels, mean free electrons per nucleon,convection zone

This page was left Blank

FACULDADE DE CIÊNCIAS DA UNIVERSIDADE DO PORTO

Abstract

Faculdade de Ciências da Universidade do Porto

Astronomy and Physics Department

Masters on Astronomy

by Liliana Novais

Compreender a origem do campo magnético nas camadas superiores do Sol e de estrelas do tipo-solar é um dos problemas mais importantes da astrofísica estelar atual. Neste estudo, investigamos como a estrutura microscópica do envelope de estrelas do tipo solar poderia criar ou suprimir os campos magnéticos observados na superfície em algumas estrelas de baixa massa. Em particular, analisamos como os níveis de ionização de diferentes elementos químicos em modelos estelares, com ou sem rotação diferencial, podem afetar a atividade magnética das estrelas.

De forma a conseguirmos estudar as estrelas em causa, utilizamos o programa *Modules for Experiments in Stellar Astrophysics* (MESA), para calcular modelos 1D para quatro estrelas, HD 10700 (Modelo A), HD 1835 (Modelo B), HD 190360 (Modelo C) e o Sol (Modelo D), que são conhecidos por terem diferentes graus de atividade magnética. A evidência observacional de atividade magnética nessas estrelas é discutida no artigo de Baliunas et al [1995].

O objetivo deste projeto foi descobrir como a evolução estelar altera a estrutura interna do envelope estelar e, por sua vez, isso afeta os níveis de ionização de diferentes elementos químicos (Hidrogénio, ^{1}H , Hélio, ^{4}He, Carbono, ^{6}C, Oxigénio, ^{8}O, Nitrogénio,^{7}N, Neon ^{10}Ne, Silício $14Si$, Magnésio, ^{12}Mg, e Ferro^{26}Fe) e a distribuição radial do número de electrões livres médios por nucleão, e a partir disso deduzimos possíveis ligações à atividade magnética da estrela.

O Sol (Modelo D) e HD 10700 (Modelo A) foram utilizados como referências para testar a qualidade de nossos modelos estelares, uma vez que estas são as estrelas melhor conhecidas neste estudo. O primeiro porque é a estrela mais conhecida e estudante que estabelece os padrões da física teórica a serem utilizados na modelação de estrelas de baixa massa, e a segunda estrela foi escolhida, uma vez que esta foi alvo de um estudo asterosismológico de Teixeira et al [2009], e, portanto, alguns dados observacionais estão disponíveis.

Descobrimos que a evolução com e sem rotação causa mudanças estruturais importantes nas estrelas, principalmente na localização e tamanho da zona convectiva, afetando a distribuição dos estados de ionização dos elementos químicos para as quatro estrelas. Igualmente, a distribuição do número médio de eletrões livres por nucleão muda significativamente nas 4 estrelas, essas diferenças podem influenciar a evolução de um ciclo magnético. A estrela HD 10700 (Modelo A) parece apresentar maiores diferenças nesta quantidade, com uma variação de até 8 %. Essas mudanças na distribuição de cargas dentro da estrela podem ser causadoras das diferenças significativas na formação e manutenção dos ciclos magnéticos nestas, resultando em ciclos magnéticos bastante distintos.

Desta forma, HD 1835 (Modelo B) é a estrela que apresenta a forte atividade magnética que tem um número médio de eletrões livres por nucleão no núcleo 20 % acima do valor encontrado para o caso do Sol (Modelo D). HD 10700 que é conhecida por não ter uma atividade magnética significativa apresenta um valor de 10 % menor do que o Sol. Finalmente, HD 19360 parece que não tem nenhuma atividade magnética, mas o número de electrões livres por nucleão presentes é idêntico ao Solar.

Além disso, também apresentamos alguns resultados de asteroseismologia. HD 10700 apresenta quase nenhuma modulação em todas as quantidades asterosismológicas calculadas: grande separação, pequena separação e segunda diferença. No caso das outras três estrelas, é possível identificar uma assinatura sísmica relacionada com a presença de rotação diferencial. HD 190360 (Modelo C) e HD 1835 (Modelo B) são estrelas de alta metalicidade com diferentes idades, os perfis são semelhantes, mas os valores para todas as quantidades calculadas são bastante diferentes. Esta poderia ser uma clara evidência de idade e resultado da evolução, ou uma evidência de sua inatividade magnética que faz seus perfis mais próximos do caso solar.

Todas as estrelas presentes neste estudo mostram diferentes estruturas internas que mudaram significativamente quando a rotação é implementada, como mencionado antes que

a região mais afetada é a zona de convecção. Essas mudanças parecem ser maiores, dependendo da idade e da metalicidade de cada modelo. As estrelas com uma metalicidade inferior parecem ser mais influenciadas por esse efeito do que as estrelas com maior metalicidade.

palavras-chave: estrelas do tipo solar, estrutura interna, evolução, rotação, asteroseismologia, níveis de ionização, electrões livres por nucleão, zona de convecção

This page was left Blank

Contents

List of Figures

This page was left Blank

List of Tables

Symbols

T	Temperature	K
r	Distance to the centre of the star	cm
R	Radius	cm
M	Mass	g
L	Luminosity	$ergs\ s^{-1}$
P	Pressure	$dyne\ cm^{-2}$
t	Time	s^{-1}
ϵ	Energy production rate	erg
ρ	Density	$g\ cm^{-3}$
G	Gravitational constant	
n_{r+1}	density of atoms in the ionization state $r+1$	m^{-3}
n_r	density of atoms in the ionization state r	m^{-3}
n_e	density of electrons	m^{-3}
G_{r+1}	Partition Function of ionization state $r+1$	
G_r	Partition Function of ionization state r	
g_e	statistical weight of the electron	
m_e	mass of the electron	g
χ_r	ionization potential of state r (to reach state r+1)	
h	the Planck constant	
k	Boltzmann constant	

This page was left Blank

Dedicated to Isabel Novais, my daughter, with all my love, so you can see the stars

This page was left Blank

Chapter 1

Introduction

Humans always gazed into the sky and asked about the nature of what they saw. Since very early in the human history we can find evidences of that interest, in places like Stonehenge and the Native American Medicine Wills, this help us to understand how important the heavens were to the early man. Technology brought us to another level and old superstitions where dropped and explained. The stars that are present in our skies seem to us almost immutable for a long time, the only records of change that we have are of supernovas that lighted the sky and scared the populations that lived at the time. They were perceived as a warning or prediction of an important event or of an catastrophe, creating panic.

Studying the internal structure of stars is a very complicated subject since one cannot look inside of them, even in the case of the Sun, our closest star, we cannot do so. Eddington, in 1920's, was one of the first astronomers to dedicate himself to this subject, and to theorise about giant stars and show that this theory could be extended to the Sun and stars similar to the Sun [1926]. He concluded this by showing that both types of stars lye along the same mass-luminosity curve, like shown in the diagram present in Figure 1.1. This allowed astronomers to conclude that stars could be studied by the ideal gas law, even if they are more dense, bringing the study of stellar constitution into mainstream astronomy.

During the 1920's, this new field emerged and became an independent one within Astronomy. Some of the names that are related to this birth are, e.g., Eddington, James Hopwood Jeans, Edward Arthur Milne, Henry Norris Russel, Svein Rossland, that, across the word, cooperated to understand the Physics and Mathematics that could describe stars. After this initial embryonic phase, a huge amount of young astronomer joined this new field and it became an important research subject.

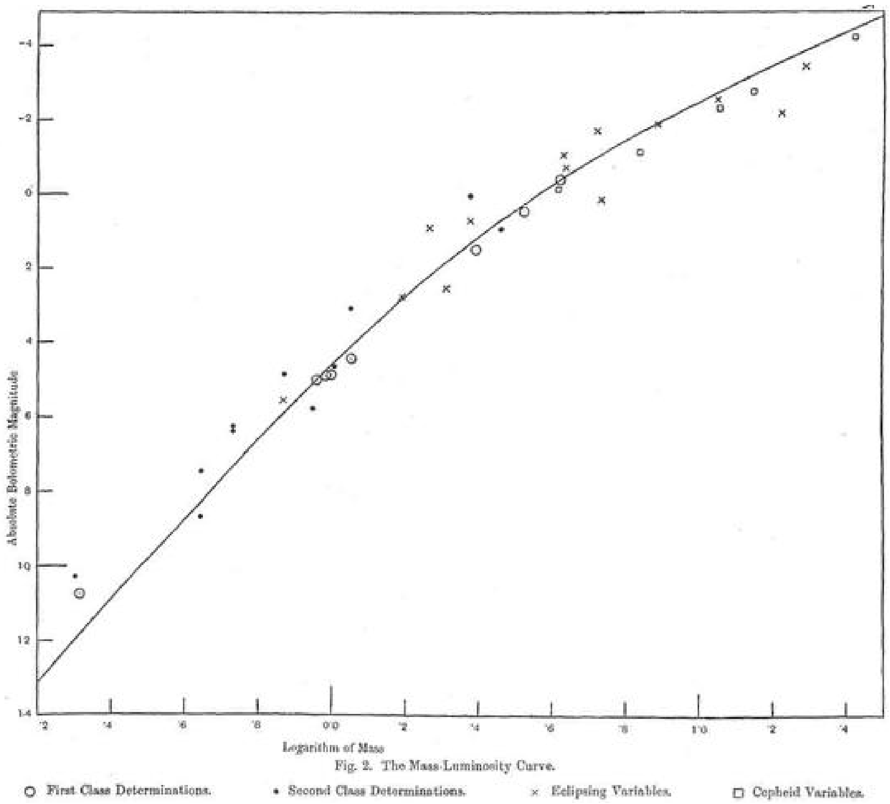

FIGURE 1.1: Mass - Luminosity relation obtained by Eddington. Taken from [?]

Even when stellar Astronomy was growing not all issues could be solved, some lasted for decades. The observational capabilities available at that time were very limited. And also, as mentioned before, there was no way that we could look inside the stars and verify that our models are accurate or not. We could only compare the results with the observational quantities available at the time for a few number of stars. It was a theoretical field that was complicated to work, since the equations where complex and only simple and classical solutions could be found.

The first revolution in this subject occurred when computers started to be used to solve numerically the structure equations, allowing astronomers to obtain more complicated and realistic solutions. But, several solutions with small divergences could explain the same observations. This problem was only solved with a second revolution that is still undergoing for the last 30 years. With the development of new technology that allowed us to observe small changes in the observational quantities, that are related to the propagation of waves in the star. Similarly to the Earth, where earthquakes allow us to understand its internal structure, the study of this oscillations allowed astronomers to have a window to the interior of stars. Technology continued to evolve and develop, helping astronomers to study in more depth the Universe, we can see further and "deeper" inside. In 1962, the first oscillations were observed by Leighton et al [1962], and latter confirmed by Evans et al [1962], giving birth to Helioseismology. With time, other stars where found to present oscillations. In order to study several these stars and to find more, a vast number of missions where developed, both on Earth (e.g. BiSon [1996], GONG [1995]) and in Space (e.g., CoRoT [2006]], Kepler [2002]).

The Sun is a middle aged star that its only special feature is that it is our closest star, this allows us to have a better knowledge and understanding of the physical phenomena that occur on it. Specially, we have a better resolution on localized solar disk phenomena, like flares, sunspots, and others. For centuries, astronomers observed closely the Sun and registered what they saw. Since Galileo, that the number of sunspots have been registered and studied, as seen in Figure 1.2.

We know that the solar spots are related with the existence of the solar magnetic field and that they are a direct proof of its existence, so this record allow us to map the variation of magnetic activity of the Sun. If we observe Figure 1.2, we can see that it is periodic, this means that the solar magnetic sunspot cycle lasts around 11 years, another important result is that it varies in amplitude. It is important to notice that there is a gap in activity that lasted about 75 years. This is not a gap on observations, but a period of low activity, during which, almost, no sunspots where observed in the solar disk. This

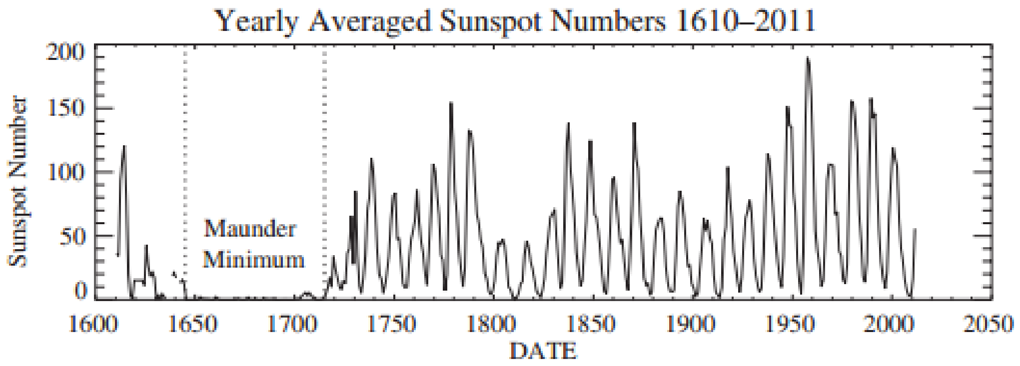

FIGURE 1.2: The early averaged sunspot number from 1610 to 2011,we can observe the 11-year cycle with long term modulation. From 1645 to 1715 we can observe the period called Maunder Minimum. This figure was taken from [1976].

period is called the Maunder Minimum (e.g., [2014], [1976]). And the mechanism that was responsible by it is still unknown.

Baliunas et al. [1995] presented a paper, were they studied the magnetic activity on nearby solar-type stars. In their work, they observed 111 stars and recorded the results obtained on the observation of the CaII line, which allow us to measure the magnetic activity of a given star. Emission in the core of the Ca II H and K resonance lines (396.8 nm and 393.4 nm) reflects non-thermal heating in the chromosphere that produces bright plages, and is perhaps the most widely used of these activity diagnostics. They concluded that solar-type stars present a vast kind of magnetic activity, some had longer cycles than the Sun, others had cycles with the same length of the Sun, others, shorter periods, and finally another group of stars presented no activity what so ever. So, what is the difference on this stars that give us different results? All of them belong to the same type, and similar spectral class, or very close between them.

In this Thesis, we chose three different stars from Baliunas paper [1995] to model, they are HD 1835, an young star with high metallicity presenting a high magnetic activity, HD 10700, an old star with low metallicity presenting no magnetic activity and HD 190360, also an older star but with high metallicity presenting no magnetic activity. The first one has an high activity and a cycle of 9.1 years, that was obtained after removing a linear trend, and filtering, according to the authors. The other two have no magnetic activity recorded, so they could be in a Maunder Minimum phase. Parallel to the modulation, I used the program MESA [2013] with the package GYRE for Asteroseismology to understand better the internal structure of each of them.

According tho Magnetohidrodynamics the Solar Magnetic Field is created deep inside the Sun, by a magnetohidrodynamical dynamo [2014]. This mechanism converts the plasma's kinetic energy into magnetic energy. This field inverts its polarity during a sunspot cycle so it lasts 22 years to recover its polarity. The source of the dynamo is located in the convection zone, most likely in a region called tachocline. Nevertheless, the chemical elements inside stars are in their ionized states. How they are distributed allow us to understand the internal structure of the star and to compare it with the one present when we implement rotation on them, and for this reason also magnetic field [2014]. The Saha equation give us the result we need to understand how ions are distributed in the stellar interior depending on the density and temperature.

In Chapter 2 we are going to present the theoretical background of this thesis that helped to build the models and the programs used to develop and test the different scenarios and obtain the models for each star. After, in Chapter 3, the results for non-rotating models are presented. The comparison between these models and the ones with rotation is made in Chapter 4. Finally, in Chapter 5 we make some concluding remarks and present future work to be done on this subject.

Chapter 2

Stellar Models and Asteroseismology in solar-like stars

The study of stars and their properties is an important field in astronomy, and the knowledge we have is vast, but there are still a lot of unsolved problems and thing we simply do not know and that we do not understand at all.

Stars come in different shapes and sizes. There are stars smaller than our Sun, and others that are so big that defy our imagination. The stars that we are going to study in this thesis are called solar-like stars because they are very similar to our Sun, the star we know better due to its close proximity. The solar-like stars present a convection zone so as expected, they present oscillations that are excited by the turbulent convection in the outer regions of the star. They should present both p- and g-modes that are exited over a range of frequencies, only varying in amplitude.

2.1 Solar-like stars

The Sun is the most important star for us since it is the one that is responsible for our existence, without it we could not exist. It is the closest star that we have and we revolve around it. Despite this fact, the Sun is not a special star, it is a ordinary G2V star, see for instance in Priest [2014]. It is in the middle of its predicted live span with about $4.6 \times 10^9\ yr$ [2014]. The HR Diagram represented in Figure 2.1 shows the position that observed stars take in the plot. Our Sun lye's in the middle of the Main Sequence, the large line-type concentration in the middle of the diagram. It is clear that stars lye in specific regions of the plot and not randomly. This led astronomers conclude that stars have specific evolutions and relations between their physical properties, such as Mass, Radius and Luminosity, that they follow no matter their small differences.

When observing the HR diagram, one can see that there are stars that are very similar to the Sun, those are called Solar-type stars or solar-like stars [1998]. Cayrel de Strobel et al. [1997] showed that the observation of these stars is important in order to understand better the properties of our own Sun when compared to them and also the habitability of exoplanets, due to the fact that Earth is the only known planet where life developed to know our Sun and understand the particularities that lead to the appearance and development of live on our planet we are able to identify possible candidates to have habitability conditions.

The classification of stars according to their similarity or difference to the Sun has evolved in time, due to the evolution of observational techniques, that allowed astronomers to obtain greater precision in their results, such as temperature, or even radius in certain cases.

The advantage of having this classification, is that one can make a comparative study of these stars to the Sun and all the knowledge that we gained for over 400 years of study and constant monitoring.

In this thesis, we studied Solar-like stars. They are defined as main-sequence stars that have a B-V colour index of 0.65, this comprises stars of a broad spectral types that go from F8V stars to K2V [1998] and that present solar-like oscillations.

Observations of the Calcium H & K line emissions of these stars allow astronomers to obtain the rotation rates, since these lines tend to rise with increasing rotational velocity

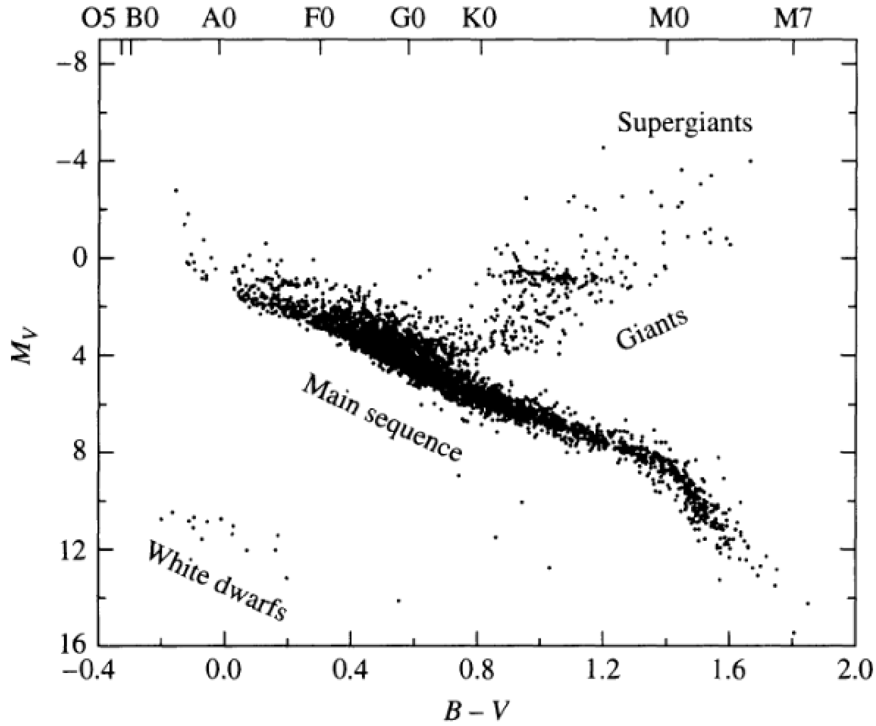

FIGURE 2.1: HR Diagram of the observed stars. We can see the main sequence, our sun is located in the middle. It is clear that the stars have lie in specific places in the diagram, just like Eddington found in the 1920's [2007]

eventually saturating in a threshold, when we have fast rotators the emission declines, and their chromospheric activity, it was observed that the behaviour between these two physical quantities is highly correlated, as concluded by Baliunas et al.[1995]. Since, these stars spin down during their evolution due to magnetic braking, one can derive their age from these observations when comparing the rotational rate obtained with the one measured for the Sun, that is used and a reference for this study, this was done for 108 solar-type stars within 52 light-years of the Sun by Mamajek & Hillenbrand [2008].

The stars that we observe have different masses and ages, resulting in internal structures that differ for each of them. We cannot look inside the stars and observe the different regions that lie on top of each other. So we need to rely on stellar structure models that have been developed for decades that describe in detail the internal structure of a given star, computing the luminosity, colour and try to predict its evolution.

One star can be modelled by two different models, depending on the final objective that one wants to achieve. Stars can be modelled as non-rotating objects, this means that we have no rotation, or we can model it, assuming that they rotate, with all consequences related to this rotation (oblateness, magnetic fields, meridional flow, and so on).

Currently, we assume that the Sun, and solar-like stars have similar internal structures. Taking into account a solar-like star in the main sequence, we can assume that its interior is divided in the following regions, as shown in figure 2.3:

- The most central region of the star is known has the core. It works as the furnace of the star and it is where all the stellar energy is created. It is considered the beating heart of the star and it is a very small region of the star occupying about 0.20 % of the entire radius.
- The radiative zone is the second most inner region of the star. Here no nuclear reactions occur. It is composed of highly ionized gas, occupying about 50% of the radius star.
- The most superficial layer is the convection zone, occupying the other 30% of the radius, here the energy is transported by convection. The top of large convection cells can be observed in the Sun, and are called granulation. Each of these cells lasts only a few minutes before it dissipate [2014].

In the base of the convective zone, there is a region that is called *Tachocline* (e.g., [2014]), where we believe that the magnetic dynamo is generated. So, understanding its nature and position inside the star is very important to fully explain the magnetic field and cycle of each stellar object.

In order to develop a model for any given star, it is required that we make some assumptions so that we can solve the structure equations:

- The star is a sphere in hydrostatic equilibrium.
- The star has spherical symmetry (only for non-rotating models, it fails when rotation is assumed, due to the oblateness effect that it causes).

- Type of atmosphere that it as.
- Convection criterion that is taken to account.
- In the centre of the star ($r = 0$), there is no singularity.

2.2 Interior of Solar-like Stars

It is important to understand how the energy is transported from the stellar interior, deep in the nucleus, where the nuclear reactions occur, to its surface.

Stars are huge reactors that produce mind-blowing quantities of energy per second. It is amazing how the balance between gravity and energy production keeps them from reaping apart in a catastrophic way.

For the purpose of this section, we need to make two considerations:

- The rate of energy flow, and hence the luminosity L, is determined by the temperature gradient and the details of energy transport,
- The luminosity of a *static* star must equal the rate at which the energy is being liberated by nuclear reactions in the stellar interior.

Since the temperature on surface is much smaller than the one on stellar centre, there is a temperature gradient, as a result, energy is transported inside the star. There are four possible ways for that transport to occur: radiative transfer, convection, conduction or neutrino emission. This last transport mechanism does not interfere with stellar matter so we are not making any considerations about it.

When energy is transported by photons that travel from hotter regions into colder ones, we have radiative transport. Conduction, on the other hand, is when the energy is transported by the particles themselves. This last one is only relevant in the degenerate electron gas case, which is not the gas in the stars in our study. When the temperature gradient becomes too large, the gas develops a instability to convection. When this happens bubbles of gas start to rise, that are hotter than their surroundings, and keep rising until they dissipate their excess heat, reaching the equilibrium with the lower-temperature environment.

The temperature gradient inside the star is given by equation 2.1.

$$\nabla \equiv \frac{d \log T}{d \log P} = \frac{P}{T}\frac{dT}{dP}, \tag{2.1}$$

where T is the temperature and P is the pressure in the considered refion. One can see that the differential equation for temperature should depend on this gradient. And all different methods responsible for the heat transport should appear, and contribute in the right weight for this equation.

Assuming the diffusive limit, we have that the energy flux, F_i, is given by equation 2.2.

$$F_i = \frac{L_r(r)}{4\pi r^2}, \tag{2.2}$$

assuming r as the distance to the stellar centre and $L_r(r)$ as the luminosity of a given region at that distance. The dependence of the opacity with temperature depends on the absorption process, and it is a function of proton's frequency. In order to solve this problem we can define the Rosseland Mean Opacity, given by equation 2.3, where B_ν is the Planck function that describes the distribution in frequency of the photons for a temperature T,

$$\frac{1}{\bar{K}} = \frac{\int_0^\infty \frac{1}{k_\nu}\frac{\partial B_\nu}{\partial T} d\nu}{\int_0^\infty \frac{\partial B_\nu}{\partial T} d\nu}. \tag{2.3}$$

In this limit we get that the temperature gradient is given by equation 2.4.

$$\nabla = \frac{L_r}{4\pi G m}\frac{P}{\rho T}\frac{1}{\bar{K}}, \tag{2.4}$$

knowing that ρ is the density, m is the mass inside the radius r, G is the gravitational constant. From the three transport mechanisms that we are considering in this thesis, the one that is less relevant in the stellar case is conduction. So, the bulk of energy transport occurs by radiative and convection mechanisms.

Let us assume, first, that the energy is transported by photons inside a given region of the star. We know that they interact with the matter that make up the star. A photon is emitted in an hotter region of the star and then it is absorbed in a colder region. So it is important to calculate the distance that it may travel before being absorbed, this quantity is called *mean free path*, l_f (as described in Figure 2.2). In equation 2.5 one can see how it relates to the absorption coefficient k_f that is the cross section of the particle of a gas with density ρ. This coefficient is also called the *opacity* of the gas, since it describes the way that the photon interacts with the gas.

$$l_f = \frac{1}{k_f \rho}. \tag{2.5}$$

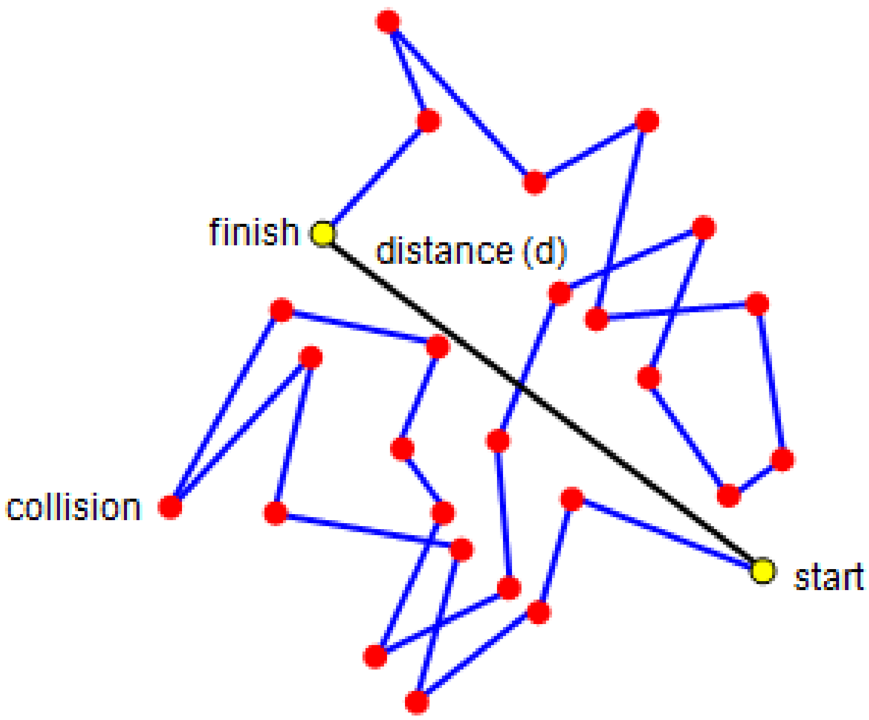

FIGURE 2.2: Mean Free Path of a particle inside a gas. As we can see it depends on the number of collisions that it undertakes. If the plasma is denser, the mean free path is shorter. Taken from `http://www.schoolphysics.co.uk/age14-16/Matter/text/Mean_free_path/index.html`.

The efficiency of this transport mechanism depends on the mediums opacity.

When we have a non rotating model the heat flux should be sufficiently great to carry out all the energy liberated within a given sphere. This implies that we have a temperature gradient. If we have a medium with large opacity, it is required a larger temperature gradient.

But, can the temperature gradient rise without any boundary? This question was answered by Scharzschild in 1906, shown in equation 2.6, where the subscript *dd* means adiabatic and the *rad* means radiative. He showed that, when the temperature gradient is too big, an instability to convections occurs as seen in Figure 2.3.

$$\left|\frac{d\ln T_{ad}}{\ln P_{ad}}\right|_{add} < \left|\frac{d\ln T}{dlnp}\right|_{rad}. \tag{2.6}$$

When we have convective motion, matter moves in a coherent and fluid way rather than as individual particles, the better form to imagine is to visualize a macroscopic mass elevating and falling in the stellar interior. As it rises, it expands. This movement continues until the two temperature gradients are equal. There is no simple solution to this problem, so it has to be calculated numerically, using the *mixing-length model*. In this model, each element in envisioned as rising or falling adiabatically for a distance, α, called the mixing length.

It is important to keep in mind that whenever convection occurs in the stellar interior, the temperature gradient is nearly adiabatic.

When we assume non-rotating stars in hydrostatic equilibrium that can be described by the four structure equations given by 2.7, 2.8, 2.9 and 2.10.

$$\frac{dm}{dr} = 4\pi r^2\rho, \tag{2.7}$$

$$\frac{dP}{dr} = -\frac{Gm\rho}{r^2}, \tag{2.8}$$

$$\frac{dL_r}{dr} = 4\pi r^2\rho\epsilon, \tag{2.9}$$

$$\frac{dT}{dr} = -\frac{Gm\rho T}{r^2 P}\nabla. \tag{2.10}$$

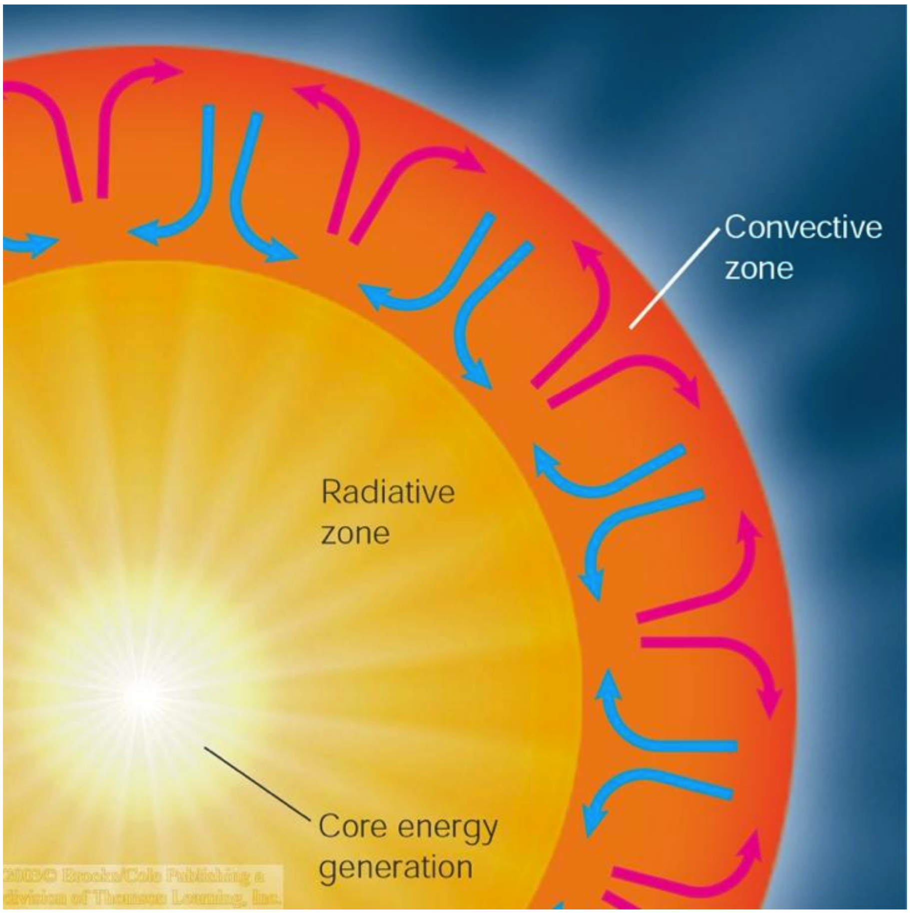

FIGURE 2.3: Schematics of the convective zone. In red we have hot plasma rising and cooling down, in blue, we have cold plasma falling and heating up (taken from `https://classconnection.s3.amazonaws.com/745/flashcards/1464745/png/stellar_structure1336016476256.png`)

With these equations and the energy transport, we can model the stars that we are going to study, using MESA to obtain the results, assuming the evolution of each star from pre-main sequence until the current accepted age.

Deep inside the stellar interior, nuclear fusion reactions are responsible by the energy prodution. In solar-like stars, during the main sequence phase, the PP chains are dominant in sunlike stars, converting hydrogen into helium. A secondary chain becomes more important in latter stages of their lives that is the CNO cycle.

Stars also present an atmosphere that lies on top of the "surface" of the star. This star is divided into several regions:

- Photosphere, the lowest and colder region of the stelar atmosphere.
- Chromosphere, this region is where the temperature of the atmosphere starts to increase.
- Transition Region, where the temperature increases abruptly.
- Corona, the hottest region of the star and also the one with the lowest density.

For the purpose of this thesis there is no need for a very elaborated atmosphere, since MESA does not implement automatically an atmosphere, we need to choose one of the available options, so we just used the "Simple photosphere" option, where no integration is done, but only an estimation for $\tau = 1/3$.

2.2.1 Impact of Rotation in Solar-like Stars

It was clear from the beginning of model building that astronomers found that younger stars move faster than older stars. This causes the firsts to have a more intense magnetic field as observed by Baliunas et al. [1995], and as mentioned by Maeder and Meynet [2000]. In Kippernhahn-Thomas model [1969], (followed in MESA) one as to take into account changes in the stellar geometry. Even if the influence of rotation is very small, for slow rotators, for instance, there are some changes in the star's thermal equilibrium [2013], this results in small fluctuations on its hydrostatic equilibrium.

The first result for these stars is that they are not spherical, but slightly oblate, this effect is more significant for fast-rotating stars. The rotation rate of a given star can be obtained from the analysis of its spectrum or the movements of active regions on the surface, this second method is more complicated for stars other than the Sun due to the large distances. Since stars are not rigid bodies, they rotate at different rates along its disk, depending on the latitude, this is known as *differential rotation.*

The rotation has a large effect on the convection, making it turbulent. It is quite different from the one described in the previous section, since the plasma carries a portion of the angular velocity of the star. When turbulence occurs through shear and rotation, the angular momentum can become redistributed to different latitudes through meridional flow.

As mentioned, the rotation acts on convection, having an important effect on the convective cells. So the criterion for stability should change in order to incorporate that effect. In fact, for rotating stars we must use the Leddoux criterion as defined in equation 2.11.

$$\nabla_{ldx} = \nabla_{ad} + \left(\frac{\beta}{4-\beta}\right)\frac{d\ln\mu}{d\ln P}, \tag{2.11}$$

where $\beta = P_g/P$ and $P = R\rho T/\beta\mu$ and μ is the mean molecular weight.

2.2.1.1 Structure equations

In order to solve the problem of symmetry that arises from the existence of rotation, one must redefine the radius coordinate of the sphere, so that it does not mean the distance to the centre, but the radius of the sphere with the same volume:

$$V_p = \frac{4}{3}\pi r_P^2 \rho. \tag{2.12}$$

Defining the radius in this way it allows the use of the mass equation in the usual way as described in 2.7, when we assume $m = m_P$ as the mass contained inside the volume that we are studying we define the surface area S_P that encloses V_P.

Also, the energy equation, is maintained the same form as assumed if it is not rotating, 2.9.

The equation of momentum balance can be written as:

$$\frac{\partial P}{\partial m_P} = -\frac{Gm_P}{4\pi r_P^4} f_P - \frac{1}{4\pi r_P^2}\left(\frac{\partial^2 r_P}{\partial t^2}\right)_{m_P}, \tag{2.13}$$

the last term is known as the inertia term. Rotation is incremented in equation 2.13 in the first term, if we take into account that:

$$f_T \equiv \frac{4\pi r_p^4}{Gm_P S_P} < g^{-1} >^{-1}, \tag{2.14}$$

where $g \equiv |\overrightarrow{g}|$ is the effective gravitational acceleration that is normal to S_P. Then, the effective temperature gradient becomes:

$$\left(\frac{\partial \ln T}{\partial \ln P}\right) = \frac{3K}{16\pi acG}\frac{P}{T^4}\frac{L_P}{m_P}\frac{f_T}{f_P}\left[1 + \frac{r_P^2}{Gm_P f_P}\left(\frac{\partial^2 r_P}{\partial t^2}\right)\right]^{-1}, \tag{2.15}$$

assuming that a is the radiation constant, k is the opacity, L_P is the energy flux through S_P. And,

$$f_P \equiv \left(\frac{4\pi r_P^2}{S_P}\right)^2 (< g >< g^{-1} >)^{-1} \tag{2.16}$$

2.3 Asteroseismology

As mentioned in Chapter 1, a huge revolution in the study of stellar structure occurred because of the discovery of small stellar quakes in the Sun by Leighton et al. [1962] in 1962 and confirmed by Evans et al. [1962]. Latter with the technological advancements several kinds of stars presented oscillations. Asteroseismology allows the study of the internal structure and the dynamics of stars. When we observe the surface of the Sun, we can see the effect that these pulsations have, since there are parts of the Sun that elevate and parts that contract. Similarly, as the case of earthquakes, astronomers can probe the interior of stars, since these oscillations travel far into the stellar centre (see Figure 2.4).

When observing the Universe, one can see that solar-like oscillations are present almost everywhere. Studying the Sun allowed us to understand and register a vast length of oscillations and to compare with the observations obtained of further stars. Helioseismology allows a better understanding of the internal structure of the Sun and this help us to understand the other solar-like stars that are assumed to present solar-like oscillations.

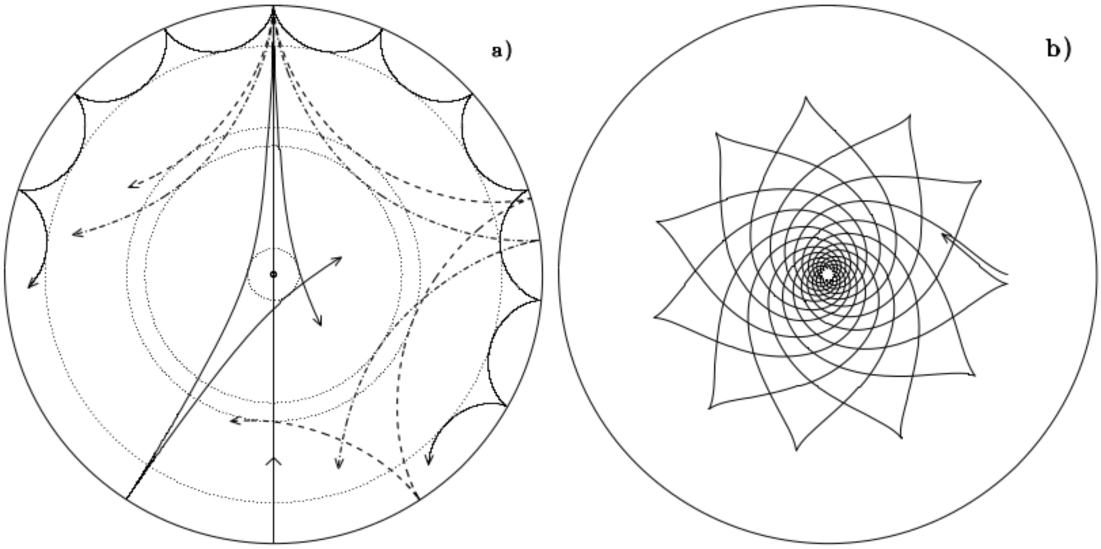

FIGURE 2.4: Propagation of rays of sound or gravity waves in a cross-section of a Sun- like star. In panel (a) we have the acoustic ray paths. And in panel (b) we have the g-mode ray path. [2010]

In order to have a deeper understanding of the internal structure of the four stars modelled in this study we are going to use asteroseismology, by applying he GYRE module available in MESA distribution.

A star is a natural oscillator, each of its different regions is sensitive to a particular frequency and this allow us to study in depth each part, high degree modes propagate in more superficial layers of the star, while high degree modes propagate deep in the stellar interior, one can observe solar-type oscillations in a vast type of stars.

If we assume that stars act like a large musical instrument it is not hard to assume hat they resonate in a given frequency, this allows us to reconstruct its shape, size and other properties just by studying the oscillation spectra.

As shown in figure 2.4 there are too many different types of waves that propagate in the stellar interior. They differ in the nature of the restoring force, so, we have the p-waves that have pressure as a restoring force and the g-waves that have gravity as a restoring force.

To study the spacial propagation we define several numbers to help us:

- $n(n = 0, 1, 2, 3, ...)$, called the radial order, that is the number of nodal surfaces in the radial direction.
- $l(l = 0, 1, 2, ...)$, called the harmonic degree.
- $m(m = -l, ..., l)$ is the azimuthal order, this is the quantity that determines the behaviour of the node in the surface of the star.

Oscillations are a powerful tool in probing the stellar interior, according to di Mauro [2017] one can obtain with high accuracy the values for their frequencies, depending only with the nature of the layer where they propagate through the stellar interior.

The origin of these oscillations depends on the type of star that we are studying. In this thesis we are centred in solar-type stars, the driven mechanism behind them is convection [2017] [1977], their amplitude is small, making them hard to detect.

Since the power spectrum of the observed oscillations can by characterized by a typical Gaussian, according to Chaplin et al. [2014], one can compute the expected theoretical value for the natural overtone of a star by computing ν_{max} for each of the stars in the study using the expression:

$$\frac{\nu_{max}}{\nu_{max\odot}} = \frac{M/M_{\odot}}{(R/R_{\odot})^2\sqrt{T_{eff}/T_{eff\odot}}} \tag{2.17}$$

According to Narayanan [2013] the value for $\nu_{max\odot}$ is 3700 μHz. The results obtained for the other stars are present in Table 3.1.

The oscillation spectrum for a given star is important, but it alone cannot give us all the information about the internal structure of each star. It is required that we compute several other quantities in order to understand better the internal organization of the star [1980].

The large separation measures the distance between consecutive modes of the same l [1990], it is related to the density of the layer where the waves propagate, it is given by the following equation, calculated for $l = 0 - 3$, so this quantity is related to the radius and mass of the star under study:

$$\Delta\nu_{nl} = \nu_{n-1l} - \nu_{nl} \tag{2.18}$$

In the case of the small difference it compares the separation of consecutive modes from adjacent degrees, it is very sensitive to the age of the star. It is given by:

$$\delta\nu_{nl} = \nu_{nl} - \nu_{n-1l+2} \tag{2.19}$$

Finally, we have the second difference, related with the ionization levels, where we compare small perturbations, this allow us to study in more depth the microphysics that dominate inside the different regions of the star, helping us to map the helium abundance in the core [2004]. It is given by the following expression:

$$\Delta_2\nu_{nl} = \nu_{n-1l} - 2\nu_{nl} + \nu_{n+1l} \tag{2.20}$$

For the purpose of this thesis, the last definition is the most important result from Asteroseismology that we can obtain. The distribution of chemical elements and ions may change the shape and distribution of this quantity changing the plot obtained.

When we implement rotation in our stellar models, their internal structure suffers some changes. So, it is important to understand how its evolutionary history affects the internal distribution. There are several quantities that are affected by it, such as, for instance, radius, mixing length, convection, meridional flow, dynamos, and so on.

Only with the use of Helioseismology we were able to start studying observationally the internal rotation of the Sun.

2.4 Microphysics of the Stellar Envelope

Due to the high temperatures that dominate in the stellar interior the atoms that make it up are in their ionized state, appearing in the fourth state of matter, called plasma. This plasma is polyatomic, since several chemical elements form stars. There are two equations that help us understand how this elements are distributed in the star, the Boltzmann and the Saha equations.

Stars are not an isolated system, they lose energy to the exterior in the form of radiation and heat, so we can not say that they are in thermal equilibrium. A new definition has to be taken into account, Local Thermodynamical Equilibrium (LTE).

When we say that a system in LTE, we are saying that although the physical properties of the given system change, the rate of that change is so slow that we can assume that, in that particular moment and in that point they remain in equilibrium with their surroundings.

Since temperatures are so high, particles are moving very fast and collisions are more likely to occur and atoms become ionized, depending on how high the temperature is plasma becomes more ionized.

One can relate the ionization level with the temperature using statistical physics. One can derive an equation that help us understand it. The Saha equation, given by 2.21, is an expression that relates the ionization state of an given element to the pressure and temperature of the medium. It arises from the combination of ideas from quantum and statical mechanics, it is used to explain the stellar spectral classification [1920], since it give us an estimate to the ionization levels in the atmosphere of the star and for this reason give us the expected spectra.

$$\frac{n_{r+1}n_e}{n_r} = \frac{G_{r+1}g_e}{G_r}\frac{(2\pi m_e kT)^{3/2}}{h^3}\exp(-\frac{\chi_r}{kT}), \tag{2.21}$$

where: n_{r+1} density of atoms in the ionization state $r+1$ m^{-3}

n_r density of atoms in the ionization state r m^{-3}

n_e density of electrons m^{-3}

G_{r+1} Partition Function of ionization state $r+1$

G_r Partition Function of ionization state r

g_e statistical weight of the electron

m_e mass of the electron g

χ_r ionization potential of state r (to reach state r+1)

T is the temperature, h is the Planck constant, k is the Boltzmann constant. This equation is very important for this thesis since we intend to study the ionization states of each chemical specie in the interior of the star. Saha equation give us the results that we need to try and understand the differences in each star.

2.5 Computation of Stellar Models

MESA is a stellar evolution code that was developed within a cooperation between different Universities and researchers [2013]. It is an open source code that every user in the community is welcome to change and develop in order to solve its particular problem and share it with the user community.

When studying stellar evolution, one needs to perform several calculations in order to obtain the evolutionary tracks of a star and to understand its internal structure, and how its global properties evolve in time. Several areas depend on the accuracy of the models developed and the results obtained. MESA computes 1D stellar structure models that help us to understand the stellar internal structure. MESA is separated in models that may be used separately.

With the advances in space astronomy, new satellites were sent to study oscillations, like CaRoT [2006] and Kepler [2002]. These missions brought to us a wide variety of light curves. With the increase of precision in the observation it became important to develop a program that would respond to this gain and that would give us more precie results. Comparing observation with the results of these models allow us to gain a better understanding on stellar interiors.

In order to solve this problem, Townsend et al. [2014] developed a code, called GYRE, that can give us the results that we need to obtain, in order to compare them to the observational values available, since it has the same precision of the satellites that operate in space. It can be used as part of MESA or in stand alone mode.

To model the stars that were studied in this thesis some coniderations had to be made. The Equation of state that was applied is delivered by the eos module. It uses as independent variables density ρ and temperature T, which are the natural variables assuming a Helmholtz free energy formulation of the thermodynamics. Even if they are assumed this way, some calculations assuming a Gibbs free energy formulation, simple root find can provide ρ given the desired $P_{gas} = P - aT^4/3$ and T.

The MESA ρ–T tables are based on the 2005 update of the OPAL EOS tables by Rogers et al [2002], and to extend to lower temperatures and densities MESA uses the SCVH tables by Saumon et al [1995].

The mixing length theory is given by the theory by Cox an Guili [1968] and given by the MLT module.

MESA does not place automatically an atmosphere in all the models, it should be placed in the inlist and the module that comands its properties is called atm module. In this module several tables with the atmospheric properties can be chosen.

The rates module contains the information about nuclear reactions that occur in the core of a given star and are based on the papers by Caughlan & Fowler [1988] (CF88) and Angulo & Aringer [1999] (NACRE).

Implementation of rotation in MESA is given by shellular rotation as defined by Meynet & Maeder [1997] and then calculate the modification to the structure equations due to the centrifugal accelaration as decribed previously. MESAstar calculates diffusion coefficients for five different rotationally induced mixing processes: dynamical shear instability, Solberg–Høiland instability, secular shear instability, Eddington–Sweet circulation, and the Goldreich–Schubert–Fricke instability. See Heger et al. [2000] for a detailed description of the physics of the different instabilities and the calculation of the respective diffusion coefficients.

Chapter 3

Computation of Models for Sun-Like Stars

3.1 Selecting the Reference Stars

In 1995, Baliunas et al [1995] published a work that was developed for several decades. In their study, the authors followed 111 solar type stars (F2-M2 spectral types) to obtain the magnetic features of each one of them.They also obtained the light curves for these stars and studied the CaII and K spectral lines that are known markers of magnetic activity. Their results are summarized in Table II of their paper [1995]. In Figure 3.1 we can observe the relative position of these stars in the HR diagram. The authors characterized stellar magnetic fields according to the magnetic cycle detected. As we can see in Figure 3.1, this activity can be very diversified. They grouped them in the following way:

1. stars without any magnetic activity (Blue Circles);
2. stars with solar-type cycles of around 11 years (Red Five Pointed Stars);
3. stars with longer periods than the Sun(Mangenta Plus signs);
4. stars with shorter periods than the Sun (Cyan Crosses);

5. stars with magnetic activity but no recorded cycle (Green Diamonds).

When studying their paper, two questions arose: "Why do solar-type stars present so different magnetic activity imprints? And why do sometimes their magnetic cycles shut-down?"

In order to try and answer these two questions, we need to choose a small sample of these 111 stars to model them, due to time limitations. The choice of those stars was made after analysing Table 2 from the Baliunas paper [1995] (represented in Appendix 8), and comparing with the page for each star available in the Simbad Astronomical [2000] and in the VizieR [2000] Databases, in order to verify the available data for each one and also the published articles on them. This allowed us to choose stars that are better studied and that have more values for the known observational quantities, also it was relevant to verify if any of them have theoretical models build in order to validate the ones developed during this thesis.

From the entire sample we choose three that have different magnetic activity imprints and started to model them. For inactive stars we chose HD 10700 (Blue circle) and HD 190360 (red circle), since they present similar ages but different metallicities, which allowed us to study the effect of metallicity in the stellar internal structure. For solar type cycle, we chose the Sun (brown five pointed star) as reference since it is the better known star. For active stars the choice was HD 1835(dark red diamond), that as an high level of activity, but this star presents a cycle similar to the Sun after post-treatment of the time-series, according to Baliunas [1995]. As we can see in Figure 3.1 all of these stars lie in very close positions in the HR diagram, so we can compare better the results.

The main features that can be studied from these stars is the effect of metallicity, age, rotation and magnetic fields in their internal structure.

When we intend to model stars that exist in our Universe and that were already studied and observed, one must have to keep in mind all the available values in the literature, that sometimes is very vast and complex. It is a long and complicated job if one has a lot of articles published about one star, that is the case for HD 10700, but, on the other

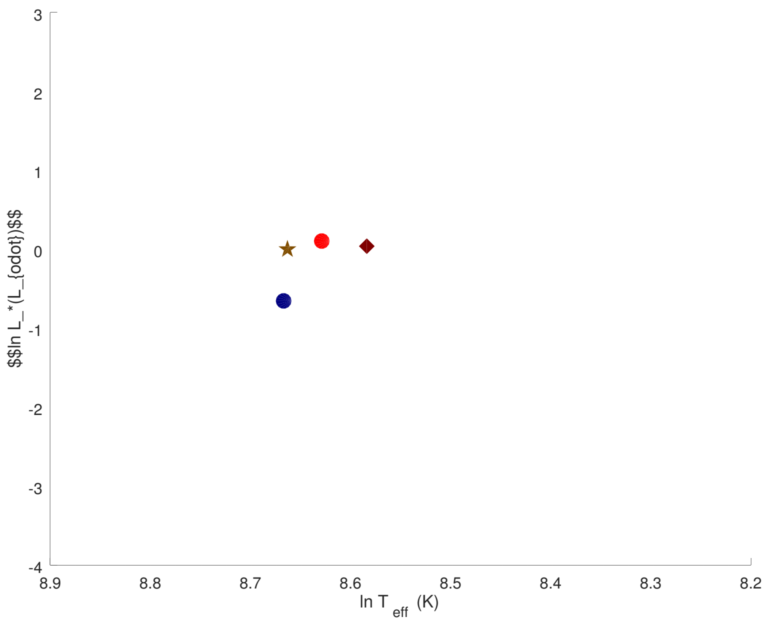

FIGURE 3.1: In this HR Diagram we have represented the 111 stars that where studied by Baliunas et al [1995]. The mangenta plus sign are stars that present longer cycles than the Sun. The cayan crosses present shorter periods than the Sun. The blue circles are stars that presented no activity what so ever. The red five pointed stars correspond to stars with solar type cycles. The green diamonds correspond to the stars that are extremelly active and with no detected cycle. There are four special symbols that correspond to the stars that were modelled in this study, these are collored inside, HD 1835 is the dark red diamond, the dark blue circle corresponds to HD 10700, the brown five pointed star is the Sun and the red circle is HD 190360.

hand, too little information about a star is also a blocker for modelling, since we cannot verify the precision of our models.

In Table 3.1 is represented a summary of some of the observational quantities available in the literature about the selected stars. From this moment on we are going to define, Model A as the model obtained for HD 10700, Model B to the model for HD 1835, Model C to the model obtained for HD 190360 and finally Model D for the Sun, that is used as a reference.

From the sample given by Baliunas et al.[1995], we have chosen three to model and study its internal structure plus the solar case:

- Sun - A G2V star [2014] at just 8 light-minutes away from us. It has 1 $M_{\odot}$ and 1 $R_{\odot}$ [2014] with an effective temperature of 5785 K, average rotational period of

26.24 days, with a sunspot cycle of 11 years. and 4.6 *Gyr* [2014].

- HD 1835 (9 Ceti) - A G3V dwarf [2006], with 0.850 Gyr [2014], only 68 light-years away [2007]. It is considered a solar analogue, with an effective temperature of 5807 K [2007], 1.09 $M_{\odot}$[2014] and 1.00$R_{\odot}$[2007]. It is a variable star with periodicity (rotational period) of 7.655 days [1996]. It is a high metallicity star with $[Fe/H] = 0.23$ dex [2012]. Stepien et al [1996], relate the variability of this star with the rotational modulation of the activity in star-spots in the photosphere, presenting a measured magnetic field with 450 G. And according to Campbell [1984] this star presents weak spectral lines for titanium oxide and calcium hydride, that, most likely, have their origin in the umbrae of star-spots, which covers around 3% of the surface of the star. According with Pavlenko et al (2002) [2012], this star presents a $log\ g = 4.47\ log(cms^{-2})$.

- HD 10700 (τ-ceti) - It is a solar analogue star, with the spectral type G8.5V [2000]. It is less massive than the Sun, with only 0.783 $M_{\odot}$ [2009] and also smaller than the Suns with 0.793 $R_{\odot}$ [2009]. It is only 12 light-years away. It is a low metallicity star $[Fe/H] = -0.55$ [2013]. It seems to be stable with low variation [1995]. This star is a close stellar system harbouring five exoplanets [2013], with one candidate that could be inside the habitable zone. It has a close age to the Sun, only slightly higher, with 5.8 Gyr [2008]. Rotational period of 34 days [1996]. Its surface gravity close to the one from the Sun, $log\ g = 4.4\ log(cms^{-2})$ [1992]. It presents a lower effective temperature than the Sun with 5344K [**?**]. It has no measurable magnetic activity [1995] and it is believed that one possible justification is that this star is a Maunder Minimum Phase, the other explanation is that we are observing this star polar-on, this i due to the fact that the cycle is detected by the variations caused by the evolution of active regions have in the stellar spectra, these regions occur very close to the equator,becoming very hard to observe and detect if we look polar-on.

- HD 190360 (Gliese 777) - This star is 52 light-years away from us, it is a G6IV class star . With a high metallicity $[Fe/H] = 0.25$. This star is in a binary, around which a jovian planet was discovered. It has about 6.7 Gyr İt is slightly bigger than the Sun with 1.13 $R_{\odot}$ and less massive with 0.96 $M_{\odot}$ and effective temperature of 5590 K and $log\ g = 4.48\ log(cms^{-2})$ [2003]. It also has no cycle present, minimum magnetic activity as showned in Table 2 from Baliunas et al. (1995). [1995]. Which makes it another possible candidate to the Maunder Minimum phase. The rotational period of this star is 38 days [2003].

Table 3.1: Available data about the stars present in this study, for the Sun we used the book from Priest [2014], Bonanno et al [2002] and Asplund et al [2008].For the other stars the references are in the text. Model A corresponds to HD 10700, Model B corresponds to HD 1835, Model C, corresponds to HD 190360 and Model D corresponds to the Sun.

Star	**Model**	**S. C.**	T_{eff} (K)	**M** ($M_{\odot}$)	**R)** ($R_{\odot}$)	$log\ g$ ($\log cms^{-1}$)	P_{rot} (days)	**M. A.**	**Age** (Gyr)	$[Fe/H]$ (dex)	ν_{max} (μHz)
HD 10700	**A**	G8.5V	5344	0.783	0.793	4.4	34	no	5.8	-0.55	4773
HD 1835	**B**	G3V	5807	1.09	1.00	4.47	7.655	yes	0.850	0.23	3996
HD190360	**C**	G6IV	5590	0.96	1.13	4.48	38	no	6.7	0.25	2849
Sun	**D**	G2V	5785	1	1	4.42	26.24	yes	4.6	0.00	3700

3.2 Building the Stellar Models

In order to model the four stars we used the Modules for Experiments in Stellar Astrophysics (MESA) [2013], each model was evolved from the *pre-main sequence*, until the accepted current age, with a time-step of 10^6 years.

The Model was calibrated using the Sun and also HD 10700, and comparing the obtain results obtained to the ones available in the literature.

For the purpose of this thesis, the more important features of the stellar structure are the top inner layers. The atmosphere is important but not that relevant, since the magnetic fields are not powered by it, but they are created inside the stars, most likely in the mentioned layers, in a region called *Tachocline* (as referred previously), located in the border between the *radiative zone* and the *convection zone*. So, for the photosphere it was chosen the use of a *"simple photosphere"*. All stars where evolved freely in time according to the structure equations described in Chapter 2. In a first approach, no rotation was added to the stars themselves. The selected input parameter used are Y_{inic}, the Helium abundance, in the original nebula that gave birth to the star, Z_{inic}, the initial abundance of Heavy Elements; α, which represents the mixing length inside the star. The stopping criterion chosen was the maximum age of the star, that is its current observed age, so that we can compare the values obtained by the model with the observational results available in the literature. The convection criterion chosen was the *Schwarzchild criterion*, due to the fact that no rotation is assumed.

To start and understand how MESA works and the available options to develop the stellar models required for the purpose of this thesis, we used the MESA Solar Model Example available in installation. As a reference for solar model results we are going to use the values available on the paper by Bahcall et al. [2006], we compared our results with the ones obtained by observations, as seen in Table 3.2. In that paper the authors also used the heavy elements abundance tables AG98 e AGS05, since they are in greater agreement with the measurements obtained by Helioseismology. The reason for the discrepancy between recent results for the abundance and the one obtained by Helioseismology is still unknown so we also followed those two tables to have a better model, closer to the results that we have available. In Table 7 of Bahcall et al. ([2006]), we have the results for the models that they build. The comparison of my results with theirs is in Table 3.2.

Table 3.2: Comparison on the Theoretical values for the tables AGS 98 and AGS 05 that Bahcall et al obtained [2006], with the values obtained using MESA.

Model	T_c	ρ_c
AG98 (theorerical)	15.67×10^6 K	152.9 gcm^{-2}
AG98 (MESA)	15.72×10^6 K	151.98 gcm^{-2}
Error (%)	0.03 %	0.6%
AGS05 (theoretical)	15.48×10^6 K	150.4gcm^{-2}
AGS05 (MESA)	15.31×10^6 K	138.28 gcm^{-2}
Error (%)	0.01 %	8%

When observing Table 3.2, one can conclude that the results using AG 98 has the smaller error in the central density, but in the central temperature is larger, but in the overall the result is better for AG98 so it was adopted for this thesis.

After doing this we used the AGS 98 tables on my model and run it with the solar values. The input data used in this model is summarized in Table 3.3.

TABLE 3.3: Input data for the Solar Calibration of the Model.

Input Data	Model D
Mass ($M_\odot$)	1
Mixing Length α	0.8
Z_i	0.09
Y_i	0.28
Age (Gyr)	4.5

The results are represented in Table 3.4, the error obtained for the observational quantities is less than 5%, so I am going to use this model as a reference for the solar one.

TABLE 3.4: Results from the Solar Calibration

Results	Model D	Observational	error (%)
T_{eff} (K)	5670.15	5785	2
L_* ($L_\odot$)	1.05	1.00	5
R ($R_\odot$)	1.02	1	2

Of the four stars in this study, as mentioned previously, the two that I used as reference to verify the accuracy of my models where HD 10700 and the Sun. If we go to Simbad and verify the number o papers available for the first, one gets over 950 references, making it a well known star.

In the paper published by Tang et al [2011], the authors made asteroseismological models of HD 10700 and we used them as a reference to compare the results that we obtained using MESA. In that paper they studied the results from two models M1 and M2, that are described in Table 4 of that paper. The input parameters for each one of the three models build is summarized in Table 3.5. Model A was developed as an average value in mass and with the age available on the literature.

It is expected that HD 10700 has a convective envelope and therefore to display solar-like oscillations. τ Ceti is the lower mass star for which solar-type oscillations has been attempted. According to Baliunas et al. [1995] this star as a rotational period of 34 days, obtained by the study of periodicities in the Ca II line. But this star is very inactive, with almost no rotational modulation. From this result there one can reach two conclusions:

TABLE 3.5: Modeling parameters from Tang et al. [2011], M1 and M2, and from the model we developed, that was developed making an average on mass of the previous two. The accepted age in the two first models is almost twice the one from my model.

Modeling Parameters	**M1**	**M2**	**A**
Mass $M/M_{\odot}$	0.775	0.785	0.7825
Mixing Length α	1.6	1.6	1.3
Z_i	0.007	0.007	0.0045
Y_i	0.253	0.243	0.26
Age(Gyr)	9.5	9.5	5.8

- Gray & Baliunas [1994] concluded that this inactivity could be related to the fact that we could be observing τ Ceti nearly polar-on.
- Judge et al [2004], on the other hand, justify that this low value of inactivity could be related to the fact that this star is in a phase similar to the Maunder Minimum Phase.

This star is a suitable target for asteroseismological studies since its radius was obtained interferometrically with an accuracy of 0.5%. Due to the vast knowledge on this star and its close proximity this makes it a great target to test evolutionary methods and models, and also to test exoplanetary search algorithms and methods.

To start implementing the data and obtaining some results to compare with the literature and check the validity of the assumptions made, we used a model without any rotation, to serve as a reference for this star and to make a comparative study, in order to find structural modifications to its interior.

It is important to have the correct initial values for the abundances of Hydrogen, Helium and heavy elements. To do so we followed the program developed from the paper by West et al. [**?**].

Using as input data the values available in Table 3.5, three models where build in order to verify the best fit for the star.

In Table 3.6 we have the results obtained using the three models in the MESA code. We can see that the model M1 is too discrepant from the observational quantities, specially

TABLE 3.6: Results obtained using the input data in table 3.5 for HD 10700 in the MESA code.

Results	Observational	M1	error(%)	M2	(%)	A	error (%)
$R/R_{\odot}$	0.793	0.747	5.8	0.788	0.6	0.826	4
T_{eff} (K)	5344	4931	7	5365	0.4	5551.65	4
$L/L_{\odot}$	0.52	0.38	26	0.45	13	0.58	11
$\log g$ ($\log(gcm^{-2})$)	4.4	4.47	2	4.53	3	4.49	1

in the luminosity where we obtained an error of 26 %. The choice for a better model is only between Model M2 and A. Although M2 presents overall a smaller error, in all observational quantities, when compared to observations, one needs to keep in mind the age of the star under study. Observationally, this quantity that is accepted by the community is of 5.8 Gyr [2008]. This fact make us discard M2, since its age is of 9.5 *Gyr*, which is much superior. So the Model A, although having a larger error it could be more accurate. If we redo model M2 using 5.8 *Gyr*, we get the results available in Table 3.7.

TABLE 3.7: Results for M2 using the accepted current age of 5.8 *Gyr*

Results	Observational	M2 (With 5.8 Gyr)	error(%)
$R/R_{\odot}$	0.793	0.723	8
T_{eff} (K)	5344	5268	1
$L/L_{\odot}$	0.52	0.40	23
$\log g$ ($\log(gcm^{-2})$)	4.4	4.56	4

Comparing the results for M2 and A using the same accepted age we can observe that A has the smaller error, specially if we take into account the luminosity of the star, where in model M2 we have a 23% of error against 11% in model A. So, we can conclude that model A, may be a better description of HD 10700 since it gives us the better values for the observational quantities. So we are assuming Model A as the better model for HD 10700.

3.3 Ionization Levels inside the stars and Asteroseismology

In this section we will present the results obtained assuming non-rotating models, for both the distribution of ionization states of the studied chemical elements inside the stars and also the asteroseismologycal results obtained with MESA and GYRE. The input data is represented in Table 3.8. Several models have been tested for each one of the stars but the ones that have a smaller error compared to the observational data where selected as the best models for each one of the stars.

It is also important to have the correct initial values for the abundances of Hydrogen, Helium and heavy elements. To do so, we again followed the program developed from the paper by West et al [**?**].

TABLE 3.8: Set of boundary conditions used to model the stars in our study.

Input Data	Model A	Model B	Model C	Model D
Mass M_{sun}	0.7825	0.93	0.96	1
Mixing Length	1.3	1.0	1.3	0.8
Z	0.0045	0.08	0.10	0.09
Y	0.26	0.27	0.28	0.28
Age (Gyr)	5.8	0.850	6.7	4.5

These parameters where inserted on the developed model in order to evolve the stars and study their internal structure. In Table 3.9, we present the results we obtained for the different models for the parameters of each star.

TABLE 3.9: Results for non-rotating Models of the four stars present int his study. By e we represent the error between observations and results obtained by the model.

Results	A			B			C			D		
	Model	Obs.	e(%)	Model	Obs.	e (%)	Model	Obs.	e (%)	Model	Obs.	e
T_{eff} (K)	5551.65	5344	4	5303.23	5807	9	5695.85	5590	2	5670.15	5785	2
L_* ($L_\odot$)	0.58	0.52	11	1.03	1.04	1	1.23	1.11	10	1.05	1.00	5
R($R_\odot$)	0.826	0.793	3	1.02	1.00	2	1.14	1.20	5	1.02	1.00	2

The four models are quite accurate with observations and are equally precise. The largest error is obtained in the Luminosity of each one. To understand how the evolution and metallicity changes the internal structure of the stars, is important to study different quantities, such as the location of the convection zone and also the ionization levels inside the star.

3.3.1 Location of the Convective Zone

There are several processes of energy transport that occur inside the star, there is one of the zones that requires our particular attention, *the convective zone.*

In Table 3.10, we have described the regions where convection occurs in each model obtained for the stars under study.

TABLE 3.10: Results for the position of the Convection Zone, for each star. The subscript *in* indicates the inner limit of the convective zone, and the subscript *out* indicates the outer limit, near the surface of the convective zone We can see that its dimension decreases with age, as expected.

Star	**Model**	R_{in}/R_*	R_{out}/R_*	%	M_{in}	M_{out}	Convection
HD 10700	**A**	0.682	0.910	22	0.768	0.782	Envelope
HD 1835	**B**	0.000	0.044	5	0.00	0.006	Core
HD 190360	**C**	0.778	1.000	22	0.902	0.909	Envelope
Sun	**D**	0.726	0.999	27	0.980	1.000	Envelope

In this thesis, we have stars in quite different stages in their evolution. In the case of Model B, the youngest star of this study, we can observe that it still presents a convective core that occupies about 5% of the central region of the star. So this means that it is in the final stages of the pre-main sequence phase and entering the Main Sequence, due to the fact that it as a very close mass to the solar case it is expected that when it reaches the Main Sequence it would not have a convective core but a radiative one. Since its mass is close to the Suns it is expected that the core would become radiative when it reaches the main sequence, and it should present a convection zone near the surface. In this model no convective zone appears at this time.

As solar type stars evolve it is expected that their convective zone would decrease with time, this is evident when comparing the other models, in the case of Model D, we have a larger convective zone then in Models C and A. For these older stars, we can observe that the core is not convective, and that there is a well-established convection zone, that varies with relative position inside the star. Models A and C do not present any observed magnetic field and the size of their convective zone is roughly the same, only varying in the position relative to the surface. In Model C it is more superficial than in Model A.

3.3.2 ^4He Abundance

It is important to keep in mind that the stars have different ages and metallicities, for this reason is important to study their abundances varies inside. We have three solar like stars with different metallicities, in Figure 3.2 we can observe the variation of ^4He as a function of the radius. If we observe the green line that corresponds to Model B (HD 1835), one

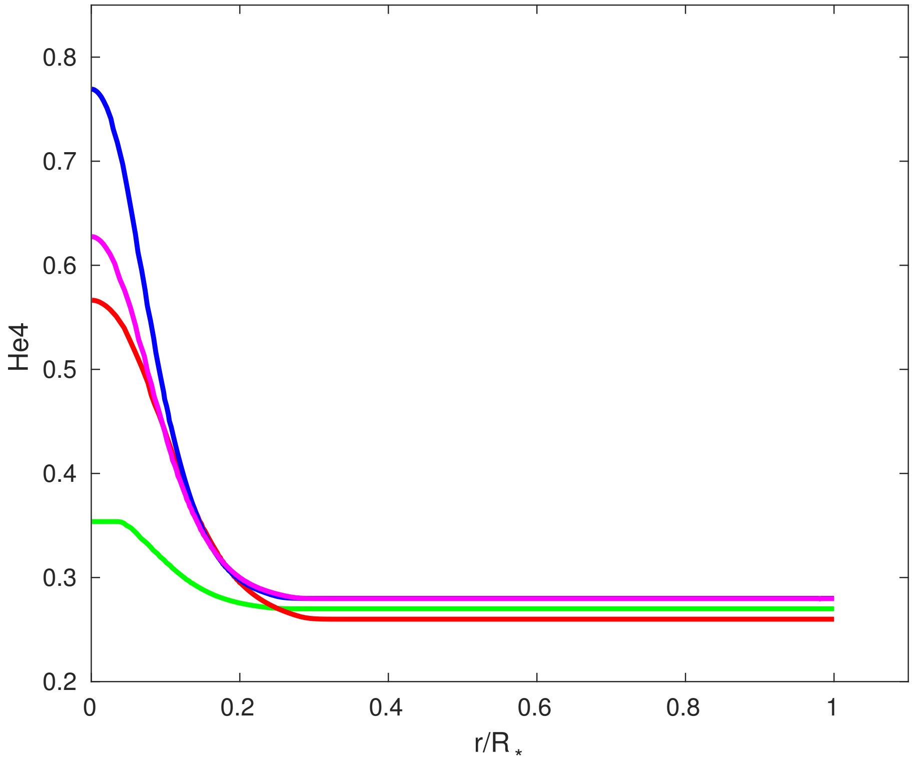

FIGURE 3.2: In this plot we can observe the abundance of Helium 4 inside each star. The stellar models are shown with the following colour scheme: Model A(Red curve), Model B (Green curve), Model C (Blue curve) and Model D (Magenta curve). The sun corresponds to Model D.

can observe that, in the core the abundance of ^4He is constant, so it can be an indicator that it still has convective core, or at least a partially convective core until about $0.05R_*$, in accordance with the results obtained in Table 3.10. It is important to see that this star as a lower abundance of ^4He than Model D (Sun), almost half the value, even if it has an higher metallicity, this is due to the nuclear reactions that occur during the life of the star, when the core converts its Hydrogen into Helium enriching the environment with Helium, increasing, this way, its abundance, this is a direct consequence of the evolution of stars.

For the case of Model A (HD 10700) it clearly has a smaller value than Model D (Sun), this may be due to the lower metallicity despite the fact that it is an older star, it had less initial value of helium, and a smaller mass that contributed to a lower abundance of this element, in its core, at that point in its evolution.

Model C (HD 10700) is the oldest star in this study, and its metallicity is higher than Model D (Sun). So it was expected that it had an higher value of ^4He, as can be seen in Figure 3.2.

From the analysis of Figure 3.2, it is clear that all stars present different abundances and internal structures that arise from their physical and chemical properties, such as age and metallicity, behaving as it was expected for each individual case. It is also clear that the evolution of stars contributes for an increase on the nuclear abundance of heavier chemical elements.

3.3.3 Ionization Levels and asteroseismology

In the interior of any star, the chemical elements are in their ionized states depending on the inner conditions present in that particular region, so we can study how they are distributed as a function of the radius. MESA software gives us the average charge of an ion at each point r (assuming that r is the distance to the center, it is a fraction of the radius), and also the mean free electrons per nucleon as a function of the radius, it is also important to study the mean free electrons per nucleon in that same region due to the fact that they could be related to the magnetic fields of the stars. So, by studying both quantities we may understand better the production and maintenance of the stellar magnetic field and also help is to probe the internal structure of that particular star.

To understand how the chemical elements are distributed inside the star and do a valid comparison, we used Model D (Sun) as a reference, as shown in Figure 3.3 and 3.3ii. It is important to keep in mind that Model A (HD 10700) is in Red, Model B (HD 1835)in Green, Model C (HD190360) in Blue and in Mangenta we represent Model D.

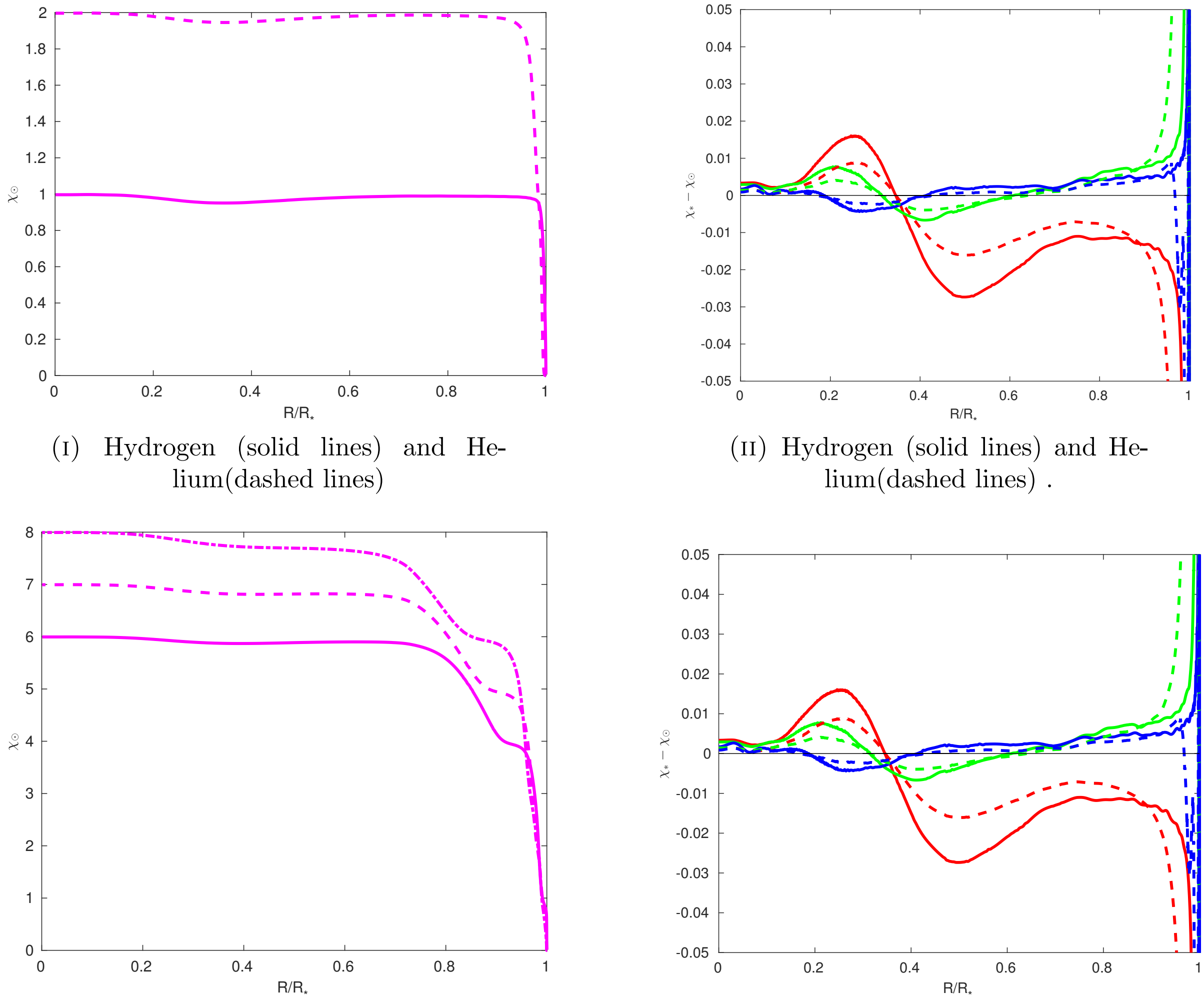

(I) Hydrogen (solid lines) and Helium(dashed lines)

(II) Hydrogen (solid lines) and Helium(dashed lines) .

(III) Carbon (solid line), Nitrogen (dashed line) and Oxygen (dot-dashed line)

(IV) Carbon (solid line), Nitrogen (dashed line) and Oxygen (dot-dashed line)

FIGURE 3.3: The panels in the left side represent the ionization level distributions in Model D (Sun). The right side panels correspond to the comparison of the Models build and Model D, Model A (HD 10700) is in Red, in green we have Model B (HD 1835) and in blue Model C (HD 190360). In this figure we represent the light elements Hydrogen and Helium, on the top two panels, in the lower panels we have the light metals, Carbon, Nitrogen and Oxygen

In Figures 3.3 and 3.4, we divided the plots into four panels. The ones on the left are the radial distribution of ionization levels for Model D. Note that these are mean values, it may be that some of the chemical elements are in higher or lower ionization states, but the mean give us back those values. In the right side, we have the comparison of the ionization levels of each star with the values of the reference model (Sun), do we can have a valid and easy comparison, seeing where it has an excess or a deficit quantifying

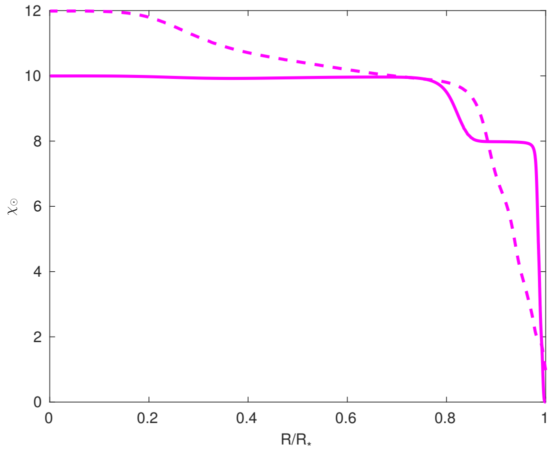

(I) Neon (solid lines) and Magnesium (dashed lines)

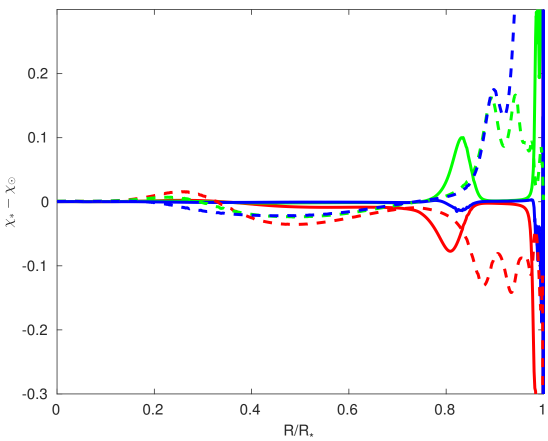

(II) Neon (solid lines) and Magnesium (dashed lines)

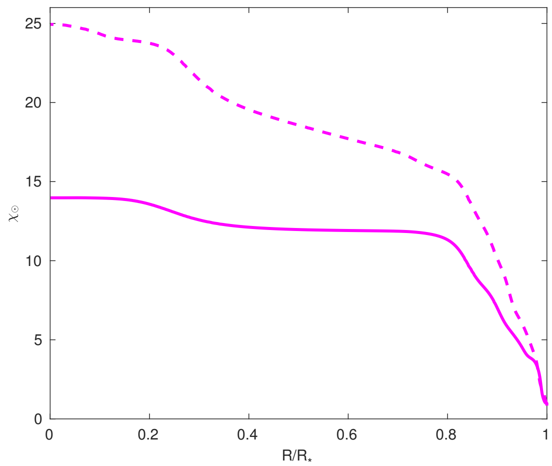

(III) Silicium (solid line), Iron (dashed line)

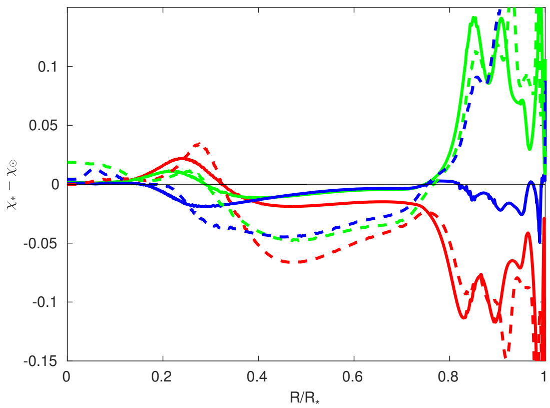

(IV) Silicium (solid line), Iron (dashed line)

FIGURE 3.4: The panels in the left side represent the ionization level distributions in Model D (Sun). The right side panels correspond to the comparison of the Models build and Model D, Model A (HD 10700) is in Red, in green we have Model B (HD 1835) and in blue Model C (HD 190360). In this figure we represent the light elements Neon and Magnesium, on the top two panels, in the lower panels we have Silicium and Iron

it. The image is truncated only showing part of the difference since we are interested in the inner regions of the star that power the magnetic fields and not on the surface, when the discrepancy is higher.

In Figures 3.3i and 3.3ii, we have represented two chemical elements, hydrogen (solid line) and helium (dashed line). In Panel 3.3i, we can easily see that both chemical elements stay in their ionization states in almost all the interior of the star, only changing in the surface. It is important to refer a small drop in this evidence between 0.2 and 0.5 R_*

where some of the ions have bound electrons decreasing the average value for ionization rates. It is clear in Panel 3.3ii that the major discrepancies between Models A, B and C with Model D start around 0.2 R_*, this position possibly marks the end of some special feature of the core of each star. We can also observe in Model A (HD 10700) that there is a region more superficial where the ionization levels are almost constant, between 0.7 and 0.95, this may mark the convection zone of the star, as previously mentioned, since convection causes this type of behaviour in the plasma that constitutes the star. For the other two stars this effect is also not that evident but it is also present, it could also be an indicator of the influence of stellar metallicity in the ionization of lighter elements. This feature is more evident in this two elements since they are very light and present a lower number of bounded electrons, which make them easier to fully ionize, making them, therefore, helpful to study the internal structure of stars. It is important to refer that Model A (HD 10700)is an apparently inactive star, observing carefully panel 3.3ii, one can see that in the most superficial region we have always a deficit in both chemical elements, also in the region were, in Model D (Sun), we have a small depression, between 0.2 and 0.4, we have an excess, this means that the chemical elements are more ionized in this small region. In the case of Model B (HD 1835), we can observe that we have an excess, in the most of the stellar radius becoming more important in the upper regions of the stellar radius. In this case there is no signature that is associated with a convection zone, as shown previously in Table 3.10, this region is absence. For Model C (HD 190360) we have a blend from the two stars, for Hydrogen we can observe a deficit until around 0.4 R_* presenting a slight effect of excess in both quantities until the most superficial regions.

Panels 3.3iii and 3.3iv correspond to Carbon (solid line), Oxygen (dashed line) and Nitrogen (dot-dashed line). It is clear that the behaviour observed in the previous panels is also present in these two with several new trends that are due to the higher number of electrons present in these elements. The largest discrepancies begin again around 0.2 R_* and extend to the outer regions of the stars where they are higher.

Assuming panels 3.4iii and 3.4ii, the chemical elements Neon and Magnesium are represented, we can observe that there is a divergence on the previous behaviour, where the discrepancies from the solar case are on the most superficial layers of the stars under study. For Model A (HD 10700)we have a deficit, for Model B (HD 1835), we have clearly an excess and finally in the case of Model C (HD 190360). When we observe panels **??** and 3.4iv, where we Silicium and Iron represented, there is a clear divergence from the solar case in the case of Models A and B, the closer case to the solar is, again, Model C.

Model B and Model C have the same metallicity but different ages, this shows that during the evolution of high metallicity stars the ionization levels become slightly lower than the Sun's, in some of the chemical elements that we have studied in this thesis. While Model A is a low metallicity star, this implies that it has a deficit in heavy elements in its plasma. The age of this star is a bit smaller than Model C, it is evident that the low metallicity stars should present a deficit on these quantities in relation to the Sun. In Figures 3.3 and 3.4, we can observe that this effect is is also present and more evident, and more visible, as we take into account lighter elements.

We know that the intensity of magnetic fields is related to the values of the charges and the free electrons present inside the star, so it is important to know how they are distributed inside of the stars. If we plot the mean free electron per nucleon obtained in MESA we can get a clearer picture of the distribution of electrons in each star as we can observe in Figure 3.5. When we want to study this values comparatively with the Sun, it is represented in Panel 3.5ii.

In Panel 3.5i, we can observe the radial distribution of the free electrons per nucleon for each of the models build. In magenta we have the solar case (Model D), as expected for Models B and C, we have an excess of free electrons due to the high metallicity that they present, on the other hand, it was expected that Model A presented a deficit in the free electrons which is clearly observed. In Model B, we can observe the effects of the convective core in free electrons distribution, due to an uniform value in the central region of the star, in the same region represented presented in Table 3.10.

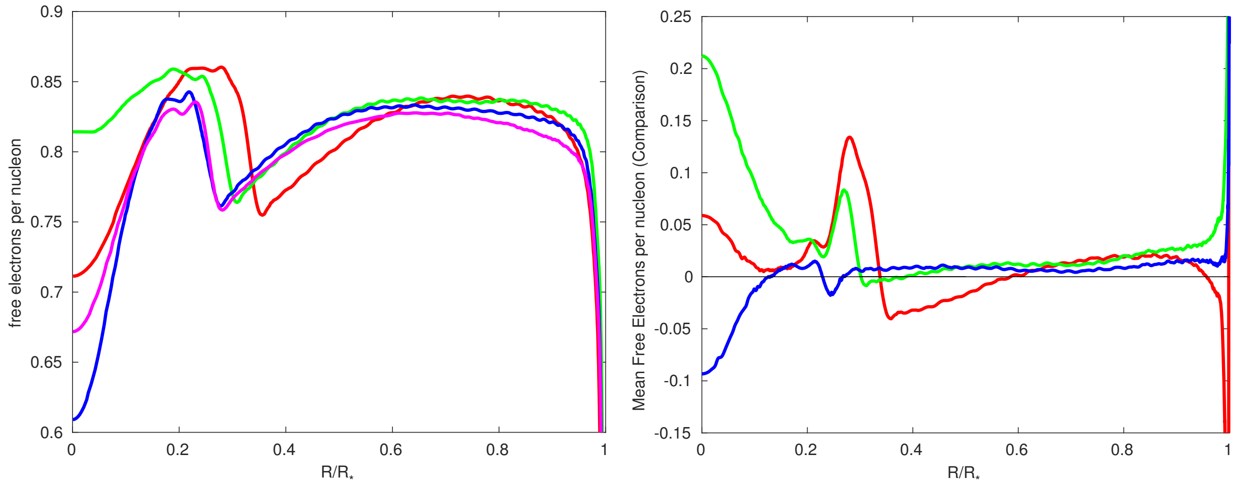

(I) free electrons per nucleon

(II) Comparison of the number of Free electrons per nucleon with the solar case

FIGURE 3.5: Mean Free Electrons per Nucleon in the stars of our study.Model A is represented in red, Model B is represented in green. Model C is represented in Blue. And, Model D is represented in Mangenta.

Comparing Models B (HD 1835) and C (HD 190360), we can see that age induces that electrons in the central regions to be bounded to the available chemical elements, in a proportion of about 10% when compared with Model D (Sun). For the case of Model A (HD 10700), the behaviour of the mean free electrons per nucleon is very different from the other models with a drastic increase in the region between 0.1 and 0.2 R_*. To have a better understanding of the divergence from Model D, one can observe panel 3.5ii, the model that is closer to the solar case is Model C, except in the inner most regions until around 0.2 R_*. While both Model B and C, present an excess of mean free electrons per nucleon in the inner most regions until around 0.35 R_*, when Model C becomes very close to the solar case while Model B present a slight decrease until around 0.4 R_*.

Comparing Models B(HD 1835) and C (HD 190360) one can assume that with age the mean free electron per nucleon decrease, since they have roughly the same metalicity. Also in the surface of the star there is an excess in the case of Model B. Model A is a low metallicity star with a smaller age than Model C, and a bit older than the Sun, as expected this star as an higher value of mean free electrons than Model C. This distribution is very different of that of the other two stars, this may be due to its metallicity, as well as its age. It is important to keep in mind that Model C is a sub-giant star with an elevated quantity of Helium on its core as we can see in Figure 3.2.

As mentioned in Chapter 2, asteroseismology allow us to understand what happens inside the stars by studying the observed oscillations from a given star. In this study only, until this moment, HD 10700 was a target for a seismological study by Teixeira et al. [2009]. This way we can, again, use this star as a reference to study the oscillations obtained for each model.

To compute the values for oscillations in Model A, we used the GYRE module and extract the values for the several oscillation modes, represented on Table 3.11.

TABLE 3.11: Observational Oscillation Modes for HD 10700, and computed Oscillation Modes using GYRE.

n	l=0			l=1			l=2			l=3		
	Obs.	**Model**	**error (%)**	**Obs.**	**Model**	**error(%)**	**Obs.**	**Model**	**error (%)**	**Obs.**	**Model**	**error (%)**
18	3293.4	3350.0	1.72									
19	3461.7	3521.3	1.72							3692.9	3754.3	1.66
20	3634.5	3693.6	1.63							3863.7	3927.6	1.65
21	3799.3	3865.8	1.75	3885.3	3948.4	1.62				4030.3	4100.9	1.75
22	3976.1	4038.4	1.57	4046.8	4121.0	1.83	4126.1	4200.0	1.79	4202.5	4274.8	1.72
23	4139.9	4219.2	1.92	4222.7	4294.3	1.70	4298.2	4373.6	1.75			
24				4388.3	4467.8	1.81	4469.5	4547.7	1.75	4545.1	4623.6	1.73
25	4481.4	4558.2	1.71									
26	4652.3	4732.2	1.72				4811.8	4896.8	1.77			
27	4816.2	4906.7	1.88	4903.1	4990.8	1.79				5060.5	5148.9	1.75
28				5072.3	5165.7	1.84	5151.8	5246.8	1.84			
29				5240.0	5340.6	1.92	5317.5	5421.9	1.97			
30				5411.2	5515.6	1.93	5492.8	5597.1	1.90			

According to Di Mauro [2017], a model can be accepted as correct if it has an error smaller than 3%. As we can observe all values obtained have an error smaller than 2%. Model A, as expected from the analysis made previously, is a good representation of the star HD 10700. As we can see from Figure 3.6, all values obtain for the oscillation modes are smaller than this value.

. Solar-type oscillations are present in this model are quite accurate with the observational values obtained by Teixeira et al [2009]. This is an important result since it allow us to conclude that the physics behind the models and that helped to build them is accurate and similar to the one that dominates the stellar interior of the real stars that are the subject of this study. Also in Teixeira et al. [2009], the authors obtained the results

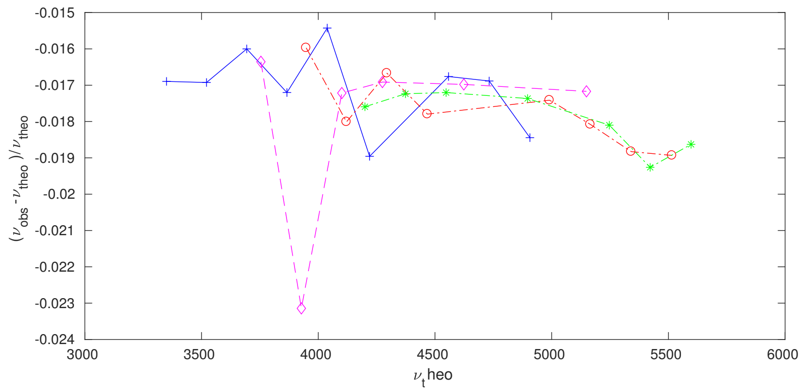

FIGURE 3.6: Comparison between observations of HD 10700 and the Theoretical values obtained with the MESA model for Model A. l=0 corresponds to the red curve, l=1 corresponds to the green curve, l=2 corresponds to the blue curve, l=3 corresponds to the magenta curve.

for large separations of each l. We can also obtain the theoretical results from model A, as shown in Table 4.4. When studying the mean large separation, one has information about the overall density of the star. As we can see the values obtained with model A are quite accurate with the observations and let us assume that the density of the star computed by MESA is close to the one present in this star.

TABLE 3.12: Values for the large separation for Model A.

Parameter	Observational Value	Theorical Value	Error (%)
$\Delta\nu_0$ (μHz)	169.6 ± 0.2	175.3	3.18
$\Delta\nu_1$ (μHz)	170.0 ± 0.3	175.2	3.06
$\Delta\nu_2$ (μHz)	170.5 ± 0.3	174.7	2.46
$\Delta\nu_3$ (μHz)	171.0 ± 0.3	174.5	2.05

Stars are natural oscillators, and they have a characteristic frequency that they resonate, depending on their physical properties. It is possible to compute the expected value for this quantity, that is described by 2.17 for each of the objects in this study. Assuming that the $\nu_{max\odot} = 3700\mu Hz$ according to Narayanan [2013], we get that for Model A we have $\nu_{max} = 4773\mu Hz$, for Model B $\nu_{max} = 3996\mu Hz$ and for Model C we have $\nu_{max} = 2849\mu Hz$. These are the natural overtones of these stars.

After computing the values for oscillations using GYRE, one can obtain the second difference (2.20), the large (2.18) and the small separations(2.19). For the purpose of this thesis we are only going to use the $l = 0$ and $l = 1$ modes for each model build.

Observing the results obtained for these quantities in Figure 4.1, one can observe that in both $l = 0$ and $l = 1$ the behaviour of the oscillations is similar, as expected. In the case of Model A (HD 10700), in red, all quantities present almost no divergence. In the case of the large separation, this is an indicator that its density does not change a lot along its radius. This is a proof that its metallicity level makes it quite different internally from the Sun, in magenta where we can observe a depression in the most superficial regions of the star. In the case of the second separation, that gives us some indication about the ionization levels present inside the star, except some small region near the surface, most star presents a low variance on this value, as viewed in Figure 3.3.

Model C (HD 190360), in Blue, presents a similar oscillation spectra as Model D, this allow us to precinct that their internal structure is similar and that the discrepancies are due to only to the effects of high metallicity and age, that changes slightly the density of the star, and the Helium abundance in the core, that is higher.

As for Model B (HD 1835), its density varies in the core, where it seems to still have a convective core, as can be seen in Figure 3.2. The core of this star seems to be smaller, as seen in the large separation plot in Figure 4.1. It presents the largest variations in the second difference, and for this reason, as expected, in ionization levels.

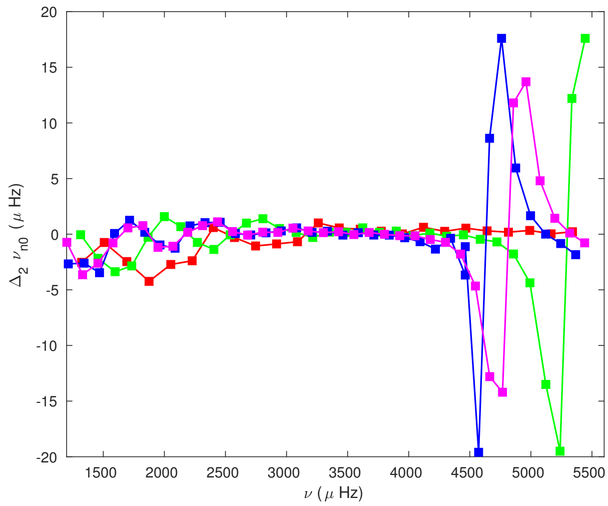

(I) Second Diference l=0

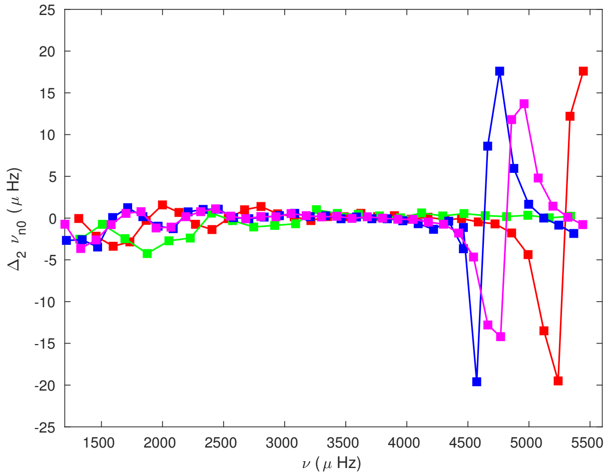

(II) Second Diference l=1

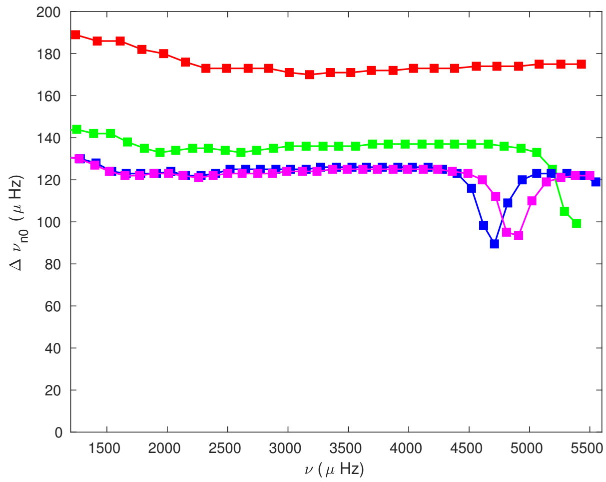

(III) Large Separation l=0

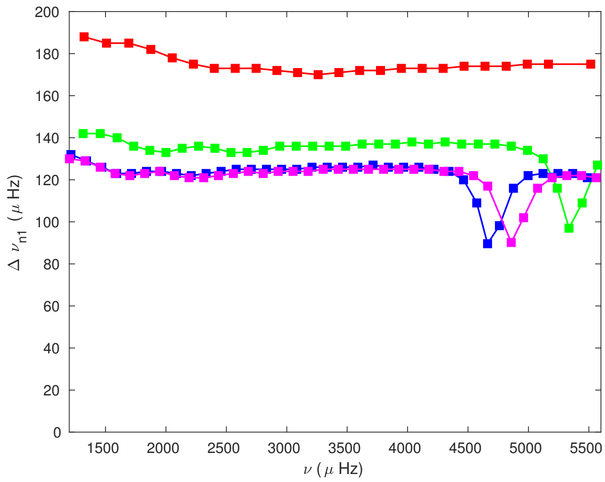

(IV) Large Separation l=1

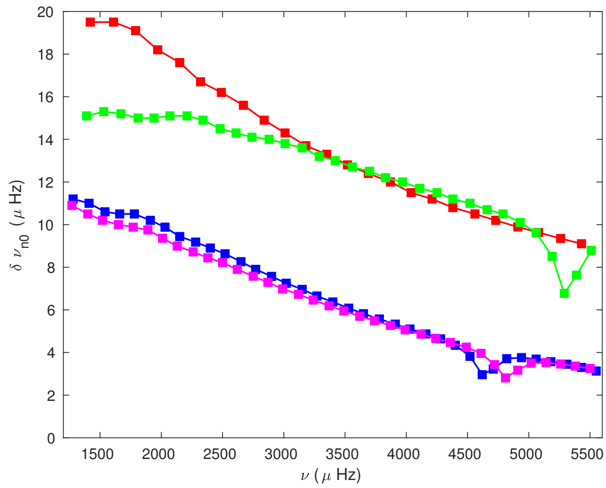

(V) Small Separation l=0

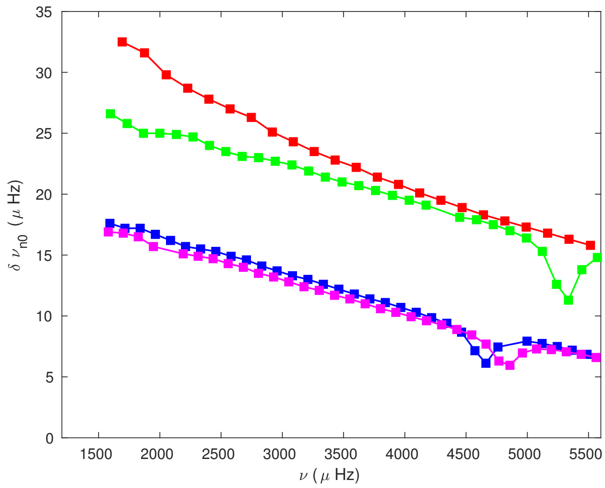

(VI) Small Separation l=1

FIGURE 3.7: Results obtained using the Gyre Module [2013], all the plots are for $l = 0$ and $l = 1$, we have the Second Difference. Model A is represented in blue, Model B is represented in red. Model C is represented in Green. And, Model D is represented in Mangenta.

For the second difference, that is related with the ionization states of the chemical elements, we can observe that in the central regions we have some signature that is related to the central discrepancies of these models as studied preciously. But the greater differences occur in the most superficial layers.

In the case of the small separation, this quantity is related with the age of the star and for these reason that in the major differences occur in the ones observed in the large separation linking the two results and the density of the region with age and the evolutionary state of the star.

3.4 Concluding Remarks

In the case of non-rotating models, we can observe that age and metalicity play an important role in the internal structure of the star. The youngest and more active star, Model B (HD 1835), presents an excess in both ionization levels and al so in the mean free electrons available in the central region of the star. This may be an indicator that this quantity is important to power and maintain the magnetic field and activity of a star. While Model C (HD 190360), which has the same metalicity presents a lower level of ionization and mean free electrons which can relate to the apparent inactivity of this star. Model A (HD 10700), is an inactive star, that presents the lowest values in this study for all quantities, this may relate to its low metalicity, causing it not to present any magnetic activity, such as it was registered by Baliunas et al [1995].

We are studying two Maunder Minimum candidates, Model A and Model C, if we study Figure 3.5 we can observe that the internal distribution of mean free electron of Model A and Model C are quite different, and the one that is closer to Model D (Sun) is the first, and in the case of Model C we have points of large discrepancy as shown in Panel 3.5ii. This could be an indicator that Model A is in the Maunder Minimum phase since it presents a deficit in mean free electrons. The case of Model C, can be more complicated, since it has an advanced age, it could be that it stop powering its magnetic cycle, and not in a Maunder Minimum Phase, due to the presence of higher values than Model D in most quantities.

Asteroseismologycal studies of the Models, let us to conclude that Model A is practically an uniform star without any modulation, as shown in Figure 4.1. This is also an indicator that it could be in a Maunder Minimum Phase. On the other hand, asteroseismologycally speaking, Model C is very similar to Model D. Observing the second separation, one can observe the oscillations and the regions of large and small separations we can relate the variations in density with the natural evolution of stars.

Chapter 4

Computation of Exploratory Models for Sun-Like Stars

Stellar rotation and the existence of magnetic fields are linked. Their influence should cause structural changes in the stellar interior.

4.1 Effects of Rotation in the Stellar Models

When implementing rotation one must take into account the effects that where described in Chapter 2. Since we want to understand how the presence of rotation and consequently the existence of magnetic fields produces changes in the internal structure of the stars, we used the models developed in Chapter 3 without any changes in the initial conditions that where described in Table 3.8, so we have no assurance that these models could be accurate and represent the real stars that were observed by Baliunas et al [1995]. To distinguish this new models from the previous ones we will add the term "rot" to each one as a subscript, so we have Model A_{rot} (HD 10700), Model B_{rot} (HD 1835), Model C_{rot} (HD 190360), and Model D_{rot} (Sun).

The Rotational profile implemented is represented in Figure 4.1i, in MESA we add the rotational profile with a code in the inlist. The routine that was implemented was the same and the differences on the profiles are only a result of the properties of each one, with particular relevance to age, following the same profile published in the paper from Amard et al. [2016], the plot were obtained from the results of the code.

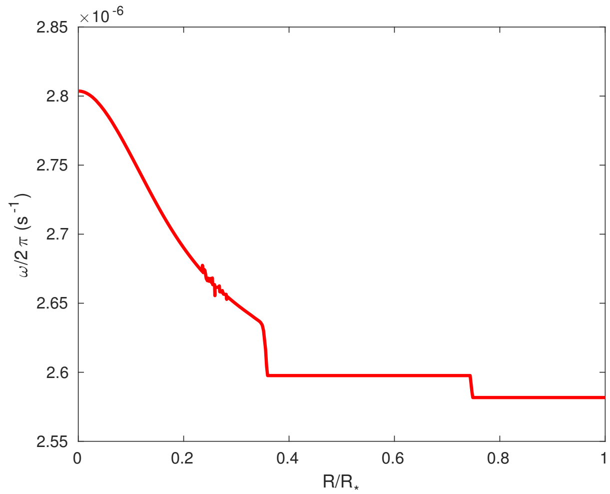

(i) Rotation profile of Model A_{rot}

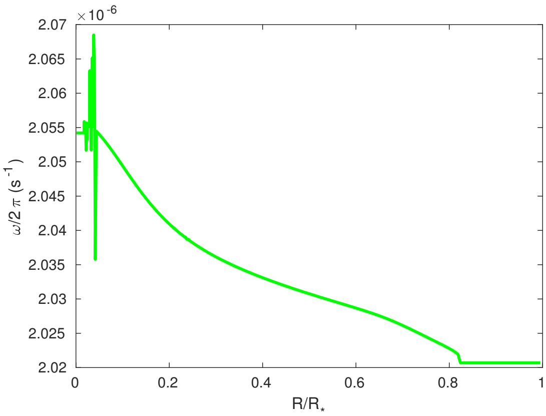

(ii) Rotation profile of Model B_{rot}

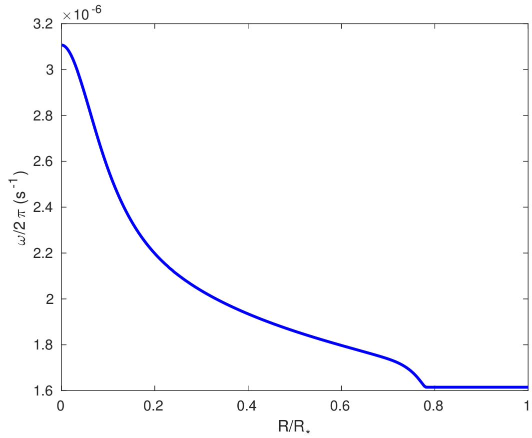

(iii) Rotation profile of Model C_{rot}

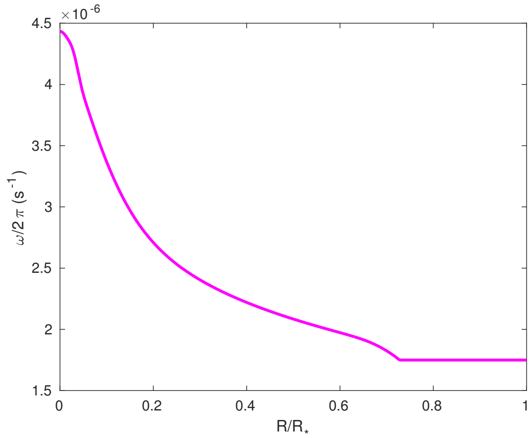

(iv) Rotation profile of Model D_{rot}

FIGURE 4.1: Rotational profile for the four models present in this study. Model A_{rot} is represented in red, Model B_{rot} is represented in green. Model C_{rot} is represented in Blue. And, Model D_{rot} is represented in Mangenta. We can see that the profile presents simmilar trends. The profiles that were implemented are in accordance with the ones obtained by Amard et al. [2016]. And they were implemented with the same routine in MESA.

Implementing rotation in the stellar models induces a magnetic field. In Table 4.1, we can observe the changes in observational quantities when we add only rotation to each one of the models build. In Model A_{rot}, the star with lower metallicity and a slow rotator, the existence of rotation reduces the values of all observational quantities, the star contracts about 3%, the luminosity decreases 17% and the effective temperature drops around 4%. Assuming Model C_{rot}, that is also a slow rotator with a high metallicity, it shows a reduction on the radius of around 6% but effective temperature and luminosity increase of 3 % and 6% respectively . Finally, in Model B_{rot}, the youngest star, with high metallicity, is the star with the fastest rotator in this study, here the radius decreases of 4% and the other two quantities increase, luminosity of 12% and effective temperature of 15 %. The changes may produce some divergences in the internal structures of each of the models, such as size of the core and convection zone, and also on the location of the last one, relatively to the surface.

From this first results that we have obtained it seems that the effects of rotation and magnetic fields of stars influence the observational quantities, such as radius, luminosity and effective temperature differently as a function of its metallicity, this means that high metalicity stars seem to increase quantities like Luminosity and effective temperature while low metalicity stars those quantities seem to decrease. This may be due to the amount of heavy elements inside of the stars, that boost this two physical properties, associating with the rotational period of each star (which is associated with its age) causes different effects on stars presenting the same metallicity but distinct ages, and thus rotational periods, being more dramatic in young solar-like stars that rotate at fastest speeds that in the case of older stars with slower rotation rates.

4.2 Location of the Convection Zone

As mentioned previously, the presence of magnetic fields should produce some changes in the position and dimensions of the convective zone. Comparing Table 3.10 and Table 4.2, one can actually see the effects that it has on each model.

Table 4.1: Comparison of the results obtained from non-rotating and rotating models with the observations. Is is clear that rotation causes changes in this quantities such as contraction of the radius, and the increase of luminosity and effective temperatures for Models B_{rot} and Model C_{rot}, while in the case of Model A_{rot} we have a reduction in all of those physical properties.

Results	T_{eff}(K)	L ($L_{\odot}$)	R ($R_{\odot}$)
Model A	5551.65	0.58	0.826
Model A_{rot}	5327.3	0.48	0.804
Obs.	5344	0.52	0.793
Model B	5303.23	1.03	1.02
Model B_{rot}	6072.4	1.16	0.973
Obs.	5789	1.04	1.00
Model C	5595.85	1.23	1.14
Model C_{rot}	5933.5	1.27	1.07
Obs.	5590	1.11	1.20
Model D	5670.15	1.05	1.02
Model D_{rot}	5713.9	1.09	1.07
Obs.	5772	1.00	1.00

Model B_{rot} (HD 1835), is particularly interesting, since, as shown in Chapter 3,it still presented a core that was partially convective. If we observe Table 4.2, we can observe that this Model, when rotation is implemented, due to the its effects it started to present a convective zone in the most superficial regions, so it clear that rotation had an effect on the macroscopic structure of this star. This may be caused by the effects of rotation and the emergence of the meridional flow. The other models are quite consistent, due to their advanced age, they do not present a convective core, and the convection zone is much more superficial and well-stablished. Assuming Model C_{rot} (HD 190360), the oldest star on this study, with an high metallicity, and the slower rotator, with a rotation period of 38 days according to the paper published by Baliunas et al. in 1996 [1996], it is possible to conclude that for this slow, high metalicity rotator, the effect of rotation in the size and position of the convective zone is negligible. For Model A_{rot} (HD 10700), we also have a slow rotator, with rotational period of 34 days, with a low metallicity, the effect of rotation in this model, is evident, there is an expansion on the dimensions of the convective zone of about 3.4%. This expansion is towards the surface of the star, making it more superficial. So it is possible to conclude that the lighter elements are more affected by rotation, and th stars with low metallicity will present structural changes more evident than high metallicity stars. In the case of Model D_{rot} (Sun), a middle aged star, with a rotational period of 27 days, the expansions is smaller, only of around 0.3%, another effect that can be observed is that the convective zone is more superficial.

From these results we can conclude that rotation has an important role on the stellar evolution and causes macroscopic structural changes in all the stars present in this study at different scales, since we can observe that the locations and size of the convection zones change when we implement rotation in our models.

Table 4.2: Location of the Convective Zone in rotating models

Star	**Model**	$\frac{R_{in}}{R_*}$	$\frac{R_{out}}{R_*}$	%	$M_{in}\ M_\odot$	$M_{out}\ M_\odot$	Convection
HD 10700	A_{rot}	0.746	1.00	25.4	0.768	0.782	Envelope
HD 1835	B_{rot}	0.829	1.00	17.1	0.997	1.00	Envelope
HD 190360	C_{rot}	0.780	1.00	22	0.90	0.91	Envelope
Sun	D_{rot}	0.727	1.00	27.3	0.982	0.998	Envelope

4.3 ^4He abundance

In the previous section, it was clear that rotation caused structural changes at the macroscopic level in the stellar interior. So it is important to see how the distribution of ^4He is also influenced by rotation. In Figure 4.2 we can see how that distribution is present in the several layers of the star.

As expected, the lower metallicity star (HD 10700) represented by Model A_{rot}, in red, shows the higher discrepancies in the distribution of ^4He from the models with and without rotation. This is clear when we observe Figure 4.2. So the internal structure of this star changes when we go deeper inside. It is clear that rotation has an higher effect in the distribution of ^4He inside low metallicity stars. We can also observe that Model B_{rot} (HD 1835) still presents a partially convective core until around 0.04 or 0.05 R_*, this means that this model presents both a convective core and a convection zone making it closer to the Main Sequence at the same age as the models without rotation.

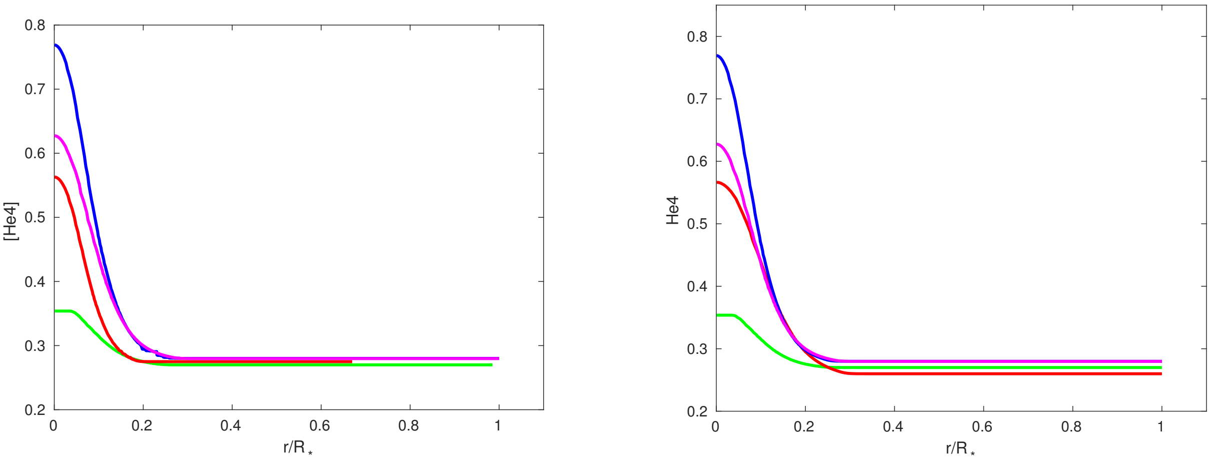

FIGURE 4.2: Abundance of ^4He in rotating models in the left panel, in the right one we have the results for the abundance of $4He$ in non-rotating models. In Red we have Model A_{rot}, in Green we have Model B_{rot}, in Blue Model C_{rot}, and finally, in Magenta we have Model D_{rot}. It is clear that in the case of Model B_{rot} there is a partially convective core even if it starts to present a convective zone as shown previously.

4.4 Ionization Levels

As seen in Chapter 3, the chemical elements that constitute the stellar plasma are in their ionization states and it only depends on the position. The existence and maintenance of magnetic fields is connected to both the ionization levels and the free electrons available inside the star.

In Figure 4.3, we have a comparison between the results in Models with rotation and the ones without rotation. We can observe how the ionization states of a given chemical element changes as a function of the radius, we can see where one is more or less ionized than the case studied previously. It is clear that the highest discrepancies occur in the surface of each model, this was expected, since the effects of rotation and magnetic fields are larger in the surface. It is also important to see that there are different behaviours in each model. Model A_{rot} (HD 10700) presents an opposite trend than Models B_{rot} (HD 1835) and C_{rot} (HD 1835),except for the case of Carbon, Nitrogen and Oxygen, since these three models vary in metallicity, one can conclude that high and low metallicity stars present opposite behaviours when we are assuming the effects of rotation and magnetic fields. In the case of Model A_{rot}, we can observe that chemical elements are less ionized than in the case without any rotation, so this implies that the electrons are more bound to the chemical elements inside the plasma. For this model, the electrons are more bound and the ionic charge of the plasma decreases that may explain the absence of a detected magnetic cycle.

For the case of Model B_{rot} we have that the chemical elements are more ionized than in the case without rotation. The exception to this behaviour is the Carbon, Oxygen and Nitrogen, as we can observe that, until around 0.75 R_*, the chemical elements are less ionized. This Model presents a clear excess of ionization in all of its radius, this implies that the charge is higher and there are more free electron that can explain the high magnetic activity.

For Model C_{rot}, we can see that the ionization levels are less divergent than in Model B_{rot}, but there is still a clear excess on the ionization levels of the chemical elements. For consistency this star should present a magnetic cycle but it is not observed. It is important to keep in mind that while the discrepancies in Model B_{rot}, are almost along all the stellar radius while, in Model C_{rot} the larger divergences occur on the most superficial regions of the star.

Finally, in the case of Model D_{rot}, only a few small differences appear in certain parts of the star. So both models are quite consistent with each other.

In Figure 4.4, we have on the left panel the distribution as a function of radius of the mean free electrons per nucleon for all models, while, on the right panel we have represented the comparison between panels 4.4i and 3.5i. One can observe that for Model A_{rot} the changes on the distribution of this quantity in bigger, with an excess on the core until 0.2 R_* and a decrease between 0.2 and 0.4 R_*. On the other hand, Models B_{rot}, C_{rot} and D_{rot} present small fluctuations, only becoming slightly larger around 0.3 R_*. On the surface this value is too discrepants. In the case of Model A_{rot} we can see that there are some discrepancies in the distribution of mean free electrons per nucleon so, this could explain the apparent inactivity of this star.

In panel 4.4ii, we can compare the results for models with and without rotation. The star that presents the greater discrepancies is Model A_{rot}, as expected from the previous

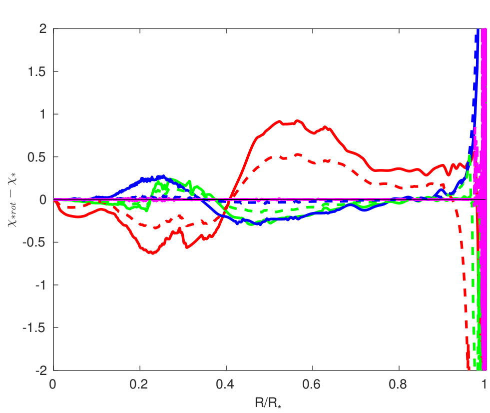

(I) Hydrogen (solid lines) and Helium(dashed lines).

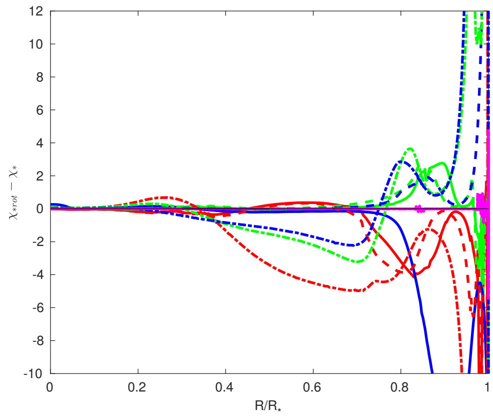

(II) Carbon(solid line), Oxygen (dot-dashed line), Nitrogen (dashed line)

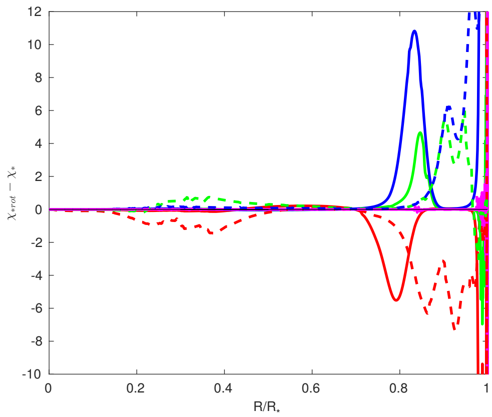

(III) Neon (Solid line), Magnesium (dashed line)

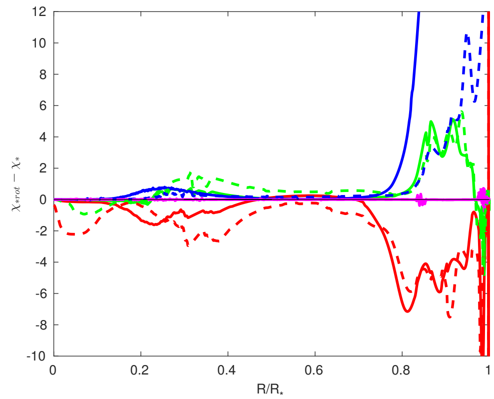

(IV) Silicium (Solid line), Iron (dashed line)

FIGURE 4.3: Comparison of ionization levels in the stars of Models with and without location. Model A is represented in red, Model B is represented in green. Model C is represented in Blue. And, Model D is represented in Mangenta.

analysis. It is clear that this model is more influenced by rotation. The other models present some fluctuations but not so dramatic as in the first case.

4.5 Asteroseismology

Like in Chapter 3, we are going to use HD 10700 as a reference star, so assuming the values obtained for asteroseismology of Model A_{rot} we can compare the results with the observational ones, that were obtained by Teixeira et al. [2009].

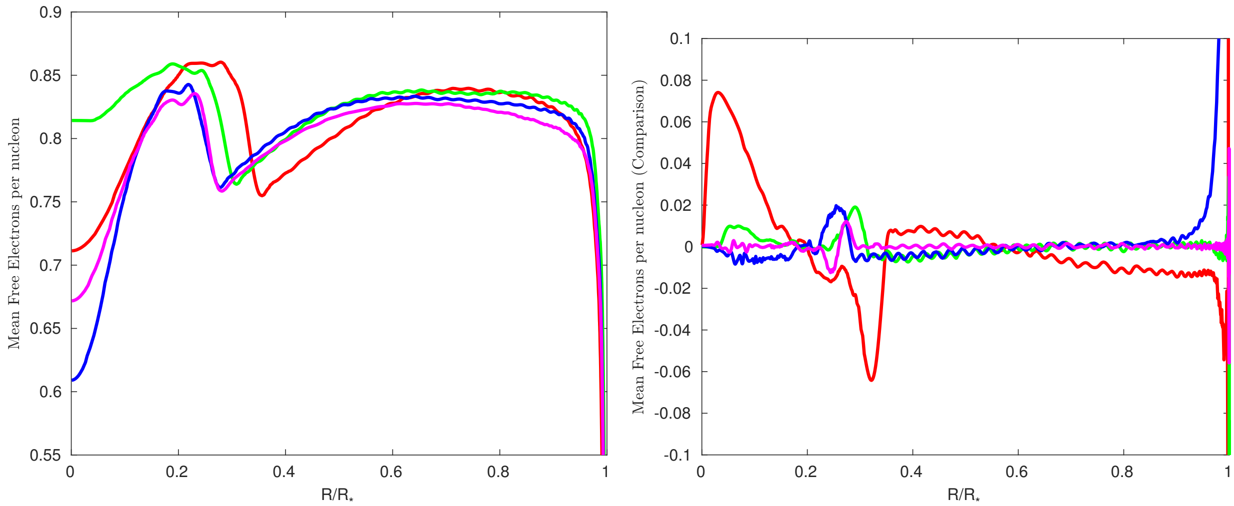

(I) Comparison of the number of free electrons per nucleon

(II) Free electrons per nucleon

FIGURE 4.4: Mean Free Electrons per Nucleon in the stars of our study.Model A_{rot} (HD 10700) is represented in red, Model B_{rot} (HD 1835) is represented in green. Model C_{rot} (HD 190360) is represented in Blue. And, Model D_{rot} (Sun)is represented in Mangenta.

TABLE 4.3: Asteroseismologycal results from Model A_rot using GYRE and observations.

n	l=0			l=1			l=2			l=3		
	Obs.	**Model**	**error (%)**	**Obs.**	**Model**	**error(%)**	**Obs.**	**Model**	**error (%)**	**Obs.**	**Model**	**error (%)**
18	3293.4	3378.1	2.57									
19	3461.7	3550.8	2.57							3692.9	3785.6	2.51
20	3634.5	3693.6	2.40							3863.7	3960.3	2.50
21	3799.3	3897.9	2.60	3885.3	3981.0	2.46				4030.3	4135.0	2.60
22	3976.1	4071.6	2.40	4046.8	4155.1	2.61	4126.1	4234.7	2.63	4202.5	4310.0	2.56
23	4139.9	4258.3	2.86	4222.7	4329.4	2.54	4298.2	4409.5	2.60			
24				4388.3	4504.4	2.58	4469.5	4584.8	2.58	4545.1	4661.2	2.49
25	4481.4	4595.3	2.48									
26	4652.3	4770.8	2.55				4811.8	4936.4	2.59			
27	4816.2	4946.4	2.70	4903.1	5031.2	2.61				5060.5	5190.5	2.56
28				5072.3	5207.2	2.66	5151.8	5289.0	2.66			
29				5240.0	5383.6	2.74	5317.5	5465.5	2.78			
30				5411.2	5560.0	2.75	5492.8	5642.1	2.71			

Observing carefully Table 4.3, we can see that rotation has an large impact in the asteroseismological results obtained with GYRE, an increase of about 1% can be observed in each of the computed modes, when comparing with the models without rotation. We expect that the same increase would happen with the other models.

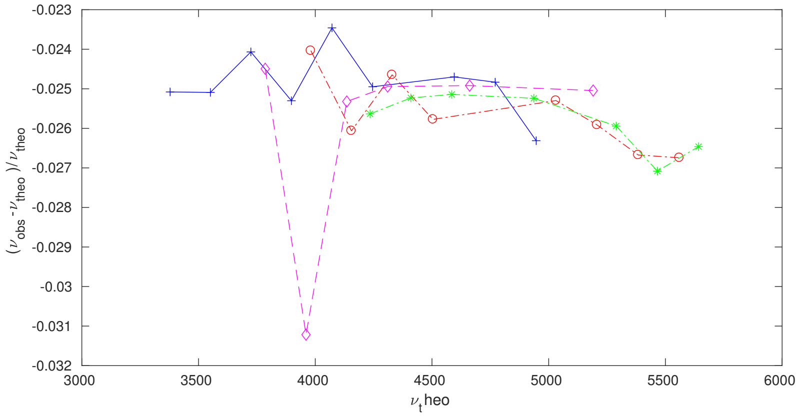

FIGURE 4.5: Comparison between observations of HD 10700 and the Theoretical values obtained with the MESA model for Model A.l=0 corresponds to the red curve, l=1 corresponds to the green curve, l=2 corresponds to the blue curve, l=3 corresponds to the magenta curve.

TABLE 4.4: Values for the large separation for Model A_{rot}.

Parameter	Observational Value	Theorical Value	Error (%)
$\Delta\nu_0$ (μHz)	169.6 ± 0.2	176.7	4.18
$\Delta\nu_1$ (μHz)	170.0 ± 0.3	176.6	3.88
$\Delta\nu_2$ (μHz)	170.5 ± 0.3	176.2	3.34
$\Delta\nu_3$ (μHz)	171.0 ± 0.3	175.9	2.87

Observing Figure 4.6, one can compare the results from the asteroseismologycal study of the models with and without rotation. The colour of each star is maintained but the results for rotating models are in full and in dashed we have the results for non-rotating models. There are small differences in the results from two types of models that arise from the small differences in the stellar internal structure.

Model A still presents no modulation and the asteroseismologycal spectra seems to be similar in both non-rotating and rotating models.

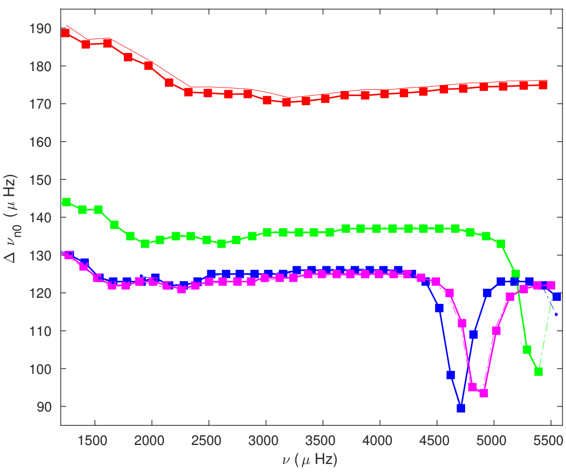

(I) Large Separation l=0

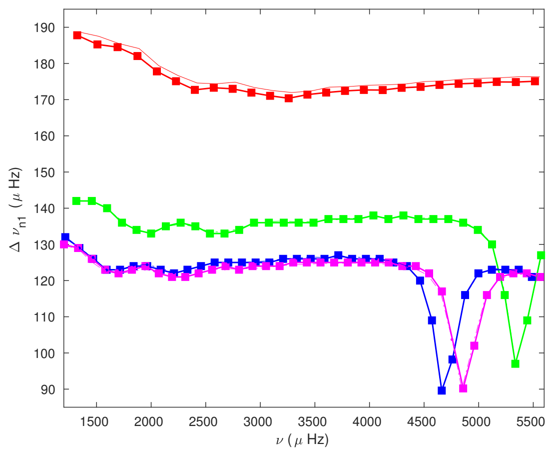

(II) Large Separation l=1

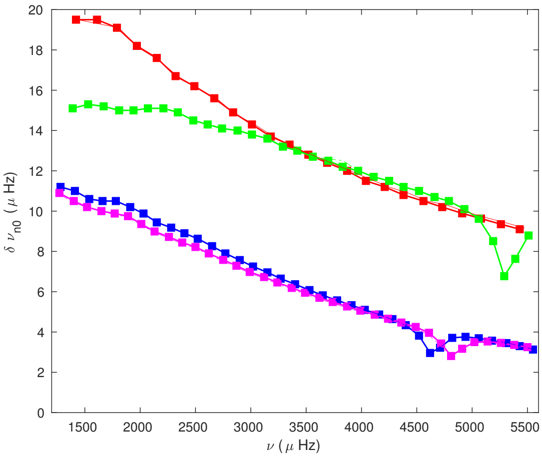

(III) Small Separation l=0

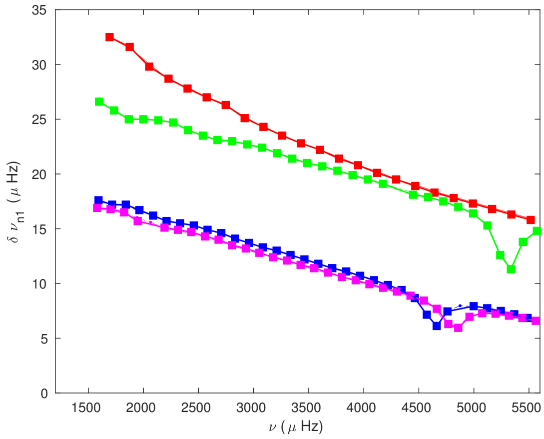

(IV) Small Separation l=1

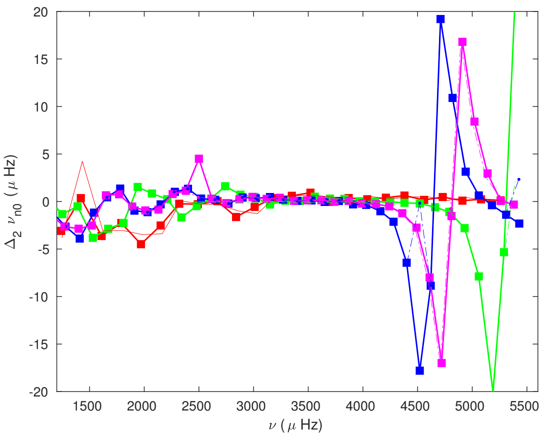

(V) Second Diference l=0

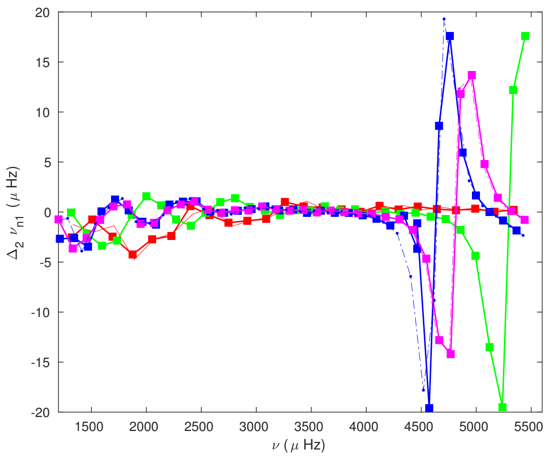

(VI) Second Diference l=1

FIGURE 4.6: Results obtained using the Gyre Module [2013]. Model A_{rot} is represented in red, Model B_{rot} is represented in green. Model C_{rot} is represented in blue. And, Model D_{rot} is represented in Magenta.using A thinner line we can see the models without rotation obtained in Chapter 3

From the previous analysis we expected that, also in asteroseismology, Model A_{rot} would present the largest discrepancies at the asteroseismology profile. As we can see in the second diference, all models present differences.

There are small differences in the second difference in all of the model due to the differential rotation that are more evident in $l = 1$ on the most superficial layers of the star.

4.6 Concluding Remarks

In this chapter, we developed exploratory models where rotation was implemented in order to understand how it influences the internal structure of the stars that we are studying, HD 10700, HD 1835, HD 190360 and the Sun. To do so, we implemented shelular rotation that is available in MESA. The rotational profiles that were implemented were validated using the paper by Amard et al [2016].

It became clear from the analysis of this result that rotation influences both stellar evolution and the stellar structure in a macro and a microscopical length.

The stars that seems to be more influenced by rotation is HD 10700 (Model A_{rot}). There could be two different explanations for this effect, the first is that the low metallicity that this star presents, so the light chemical elements are more influenced by rotation due to its lighter mass; the second possible explanation could be related with the fact that this star presents a lower mass than the other stars in this study and for this reason the effects of rotation are larger due to its small size. The obtained differences may also explain the low activity of this star, since the electrons are more bound causing a decrease on the charge of the plasma that composes the star, which may cause a decrease on the magnetic activity of the star as it was observed by Baliunas et al [1995].

Models B_{rot} and C_{rot} are high metallicity stars, the influence of rotation was not so dramatic on the second than on the first. This is due to the fact that HD 190360 is an older star, so it is in a completely different evolutionary state and they have different rotational periods, so the younger star that rotates faster presents higher discrepancies, as expected. For this reason, it is expected that this star presents a larger magnetic activity, as it was observed by Baliunas et al. [1995].

The model that presented less discrepancies was Model D_{rot}, the solar case, with only a few fluctuations. It was not as dramatic as on the other models.

Both HD 10700 and HD 190360 present simillar macroscopic internal structures, with a convective zone near the surface, but the similarities stop at this point, where we assume the distribution of free electrons and th ionization states of each chemical element both stars could not be more different. So the apparent inactivity of both stars could have different explanations other than the Maunder Minimum, or this phase could be caused by different sources.

It is clear that rotation also influences the asteroseismological results, becoming more evident in the case of HD 10700 (Model A_{rot}).

Chapter 5

Conclusion

In this study, we investigated how the microscopic structure of the envelope of sun-like stars could create or suppress the magnetic fields observed in the surface in some low-mass stars. In particular, we analysed how the ionization levels of different chemical elements in stellar models with or without differential rotation could affect the magnetic activity of stars.

We used the Modules for Experiments in Stellar Astrophysics (MESA), to compute 1D models for four stars, HD 10700 (Model A), HD 1835 (Model B), HD 190360 (Model C) and the Sun (Model D) which are known to have different degrees of magnetic activity. The observational evidence of magnetic activity on these stars is discussed in the Baliunas et al paper [1995].

Using the Sun and HD 10700 as references to test the quality of our stellar models, we were able to chose the opacity tables to use and also to calibrate our results comparing to the observations obtained by Teixeira et al. [2009], and the model build by Tang et al. [2011]. We were able to obtain a model that is more accurate with all observational data and therefore a better model for HD 10700.

In Chapter 3, we presented the results from non-rotating model, and we found that the evolution without rotation causes important structural changes in the stars, mainly in the location and size of the convective zone, affecting the distribution of the ionization states of the chemical elements for the four stars.

The core abundance of ^4He , is larger in Model C (HD 190360), as expected, due to its advanced age, but also because it has an high metallicity. Assuming Model A (HD 10700), that is a low metallicity star, and compare with Model D (Sun), we can see that even though it is an older star, the abundance of ^4He is lower, this is due to the fact that it had a lower value of this chemical element during it formation.

HD 1835 (Model B) and HD 190360 (Model C), are both stars that have similar metalicity but with completely different ages, and they are a good case study for the effects of evolution in the stellar structure. It is clear that the location of the convection zone differs in both cases. In the first star we still have a partially convective core (about 5% of all stellar radius) and on the second we have a well established convective zone closer to the surface, occupying about 22% of the total radius. So this is a proof of the effects that evolution have on the stellar internal macro-structure. Comparing the micro-structure, both in the ionization levels and the mean free electrons per nucleon, we can observe that as stars become older the electrons become more bound. In the case of HD 1835 (Model B), we have an excess of 20% of mean free electrons per nucleon in the core than the Solar case. Since this star is more magnetically active than the Sun, this could link the ionization levels and magnetic activity. In HD 190360 (Model C) we have an excess of only 5%, this proves the effect that evolution has on this quantity.

Assuming the ionization levels of all chemical elements studied, we can see that in HD 1835, the chemical elements are more ionized than in the solar case. While in HD 190360, the ionization levels from the different chemical elements inside the star are closer to the ones obtained for the Sun. We are ignoring the surface differences, since they are too high. So, this could be a hint to the different magnetic activities presented by the stars in this study.

HD 10700 (Model A), is a different case because it is a low metallicity star that as a closer age to HD 190360 (Model C), so we can compare the effects of this quantity in the internal structure. The % of the stellar radius occupied by the convective zone is the same. So this quantity seems not having an important role in this macroscopic feature of the stellar internal structure. The first star seems to have in most of its interior a lower ionization level than the Sun, so the effect of metallicity is important in the ionization levels of each chemical element present in the stellar interior. Becoming higher or lower than the Solar case depending on it the star has more or less metals. The number of mean free electrons is also lower than in the solar case for HD 10700 (about 8%), as expected from the previous result.

So, the distribution of mean free electrons per nucleon changes significantly for the 4 stars, these differences may influence the evolution of a magnetic cycle. These changes on the distribution of charges inside the star, may be responsible by significant differences in the formation and maintenance of the magnetic cycles among stars, resulting in quit distinct magnetic cycles.

Accordingly, HD 1835 (Model B) is the star that present the strongest magnetic activity that has a mean free electron per nucleon in the core 20% above the value found for the Sun. HD 10700 (Model A) that is known to not have a significant magnetic activity presents a value of 10% lower than the Sun. Finally, HD 19360 (Model C) seems that also do not have any magnetic activity, but presents mean free electrons per nucleon closer to the Suns. This gives us a hint that these last two stars apparent inactivity could be related to this distribution.

Also in Chapter 3, we present the results for an asteroseissmologycal study of the stars. Assuming HD 10700, as a reference, we obtained an error of less than 2% in each mode, so we can conclude that the model obtained for this star is a good approximation, and that our assumptions are close to the real star. So we can extrapolate that it is also for the other two stars.

HD 10700 presents almost no modulation in all computed asteroseismic quantities: large separation, small separation and second difference. In the case of the other three stars, it is possible to identify a seismic signature related with the presence of differential rotation.

HD 190360 and HD 1835 are high metallicity stars with different ages, the profiles are similar but the values for all computed quantities are quite different. This could be a clear evidence of age and a result of evolution, or a evidence of their magnetic inactivity that makes their profiles closer to the solar case, as seen for HD 190360 (Model C).

The rotational models presented in this study are purely theoretical and were used only as a study of the effects qualitatively, there is still future work to be done in this area.

Rotation influences the location and size of the convective zone, making it more shallower and slightly larger. In the case of HD 1835, we can observe that it still presents a convective core but it also has a small convection zone near the surface. So the evolutionary phase that a given star is in is affected by rotation.

Assuming both the ionization levels and the mean free electrons per nucleon, we can see that there are differences on the micro-structure of each star.

In the case of HD 10700, both types of model, with and without rotation, are similar, with the same trends, but when implementing rotation in them, the error when compares with the asteroseismological observations increases (up to almost 3%), this implies that there should be a refinement on the initial input parameters.

All stars present in this study show different internal structures that changed significantly when rotation is implemented, as mentioned before the most affected region is the convection zone.

From this study we can conclude that rotation changes some of the physical properties of the star influencing the magnetic fields that they present. Model B (HD 1835) is a young star and the emergence of a magnetic cycle is an indicator that it is entering the Main Sequence Phase. Model A (HD 10700) and C (Hd 190360) are older stars that do not present any magnetic cycle, for the case of Model C_{rot} we have that the mean free electrons per nucleon are not highly influenced by rotation, only a few fluctuation emerge, on the other and the ionization levels of the chemical elements seem to more influenced by it. These two stars are candidates to be a Maunder Minimum phase, this study do not let us conclude if there is a particular reason for the apparent inactivity of this star rather made us think if this phase could be caused by several processes, not only one single reason.

For the case of HD 190360 (Model C), since it is very similar to the Sun, its apparent inactivity could be related to a Maunder Minimum Phase.But in HD 10700 the response is not so clear because this star is very different from the solar case

In this work we have shown that the ionization levels and the amount of free electrons could be linked to the magnetic activity of stars. Moreover, it is possible that the changes on the structure of stars due to rotation and presence of magnetic fields could affect the eigenfrequencies of stellar acoustic modes.

In order to have a better understanding of the results more models should be build for the stars present in the paper from Baliunas et al [1995].

Bibliography

[1] L. Amard, A. Palacios, C. Charbonnel, F. Gallet, and J. Bouvier. Rotating models of young solar-type stars. Exploring braking laws and angular momentum transport processes. *aap*, 587:A105, March 2016.

[2] C. Angulo, M. Arnould, M. Rayet, P. Descouvemont, D. Baye, C. Leclercq-Willain, A. Coc, S. Barhoumi, P. Aguer, C. Rolfs, R. Kunz, J. W. Hammer, A. Mayer, T. Paradellis, S. Kossionides, C. Chronidou, K. Spyrou, S. degl'Innocenti, G. Fiorentini, B. Ricci, S. Zavatarelli, C. Providencia, H. Wolters, J. Soares, C. Grama, J. Rahighi, A. Shotter, and M. Lamehi Rachti. A compilation of charged-particle induced thermonuclear reaction rates. *Nuclear Physics A*, 656: 3–183, August 1999.

[3] M. Asplund. Improved age estimation for solar-type dwarfs using activity-rotation diagnostics. *Astrophysical Journal*, 687:1264–1293, November 2008.

[4] A. Baglin, M. Auvergne, L. Boisnard, T. Lam-Trong, P. Barge, C. Catala, M. Deleuil, E. Michel, and W. Weiss. CoRoT: a high precision photometer for stellar ecolution and exoplanet finding. In *36th COSPAR Scientific Assembly*, volume 36 of *COSPAR Meeting*, 2006.

[5] J. N. Bahcall, A. M. Serenelli, and S. Basu. 10,000 Standard Solar Models: A Monte Carlo Simulation. *apjs*, 165:400–431, July 2006.

[6] S. Baliunas, D. Sokoloff, and W. Soon. Magnetic Field and Rotation in Lower Main-Sequence Stars: an Empirical Time-dependent Magnetic Bode's Relation? *apjl*, 457:L99, February 1996.

[7] S. L. Baliunas, R. A. Donahue, W. H. Soon, J. H. Horne, J. Frazer, L. Woodard-Eklund, M. Bradford, L. M. Rao, O. C. Wilson, Q. Zhang, W. Bennett, J. Briggs, S. M. Carroll, D. K. Duncan, D. Figueroa, H. H. Lanning, T. Misch, J. Mueller, R. W. Noyes, D. Poppe, A. C. Porter, C. R. Robinson, J. Russell, J. C. Shelton, T. Soyumer, A. H. Vaughan, and J. H. Whitney. Chromospheric variations in main-sequence stars. *Astrophysical Journal*, 438: 269–287, January 1995. doi: 10.1086/175072.

[8] S. Basu and H. M. Antia. Constraining Solar Abundances Using Helioseismology. *apjl*, 606:L85–L88, May 2004.

[9] N. M. Batalha, J. Jenkins, G. S. Basri, W. J. Borucki, and D. G. Koch. Stellar variability and its implications for photometric planet detection with Kepler. In B. Battrick, F. Favata, I. W. Roxburgh, and D. Galadi, editors, *Stellar Structure and Habitable Planet Finding*, volume 485 of *ESA Special Publication*, pages 35–40, January 2002.

[10] A. Bonanno, H. Schlattl, and L. Paternò. The age of the Sun and the relativistic corrections in the EOS. *aap*, 390:1115–1118, August 2002.

[11] D. W. Kurtz (auth.) C. Aerts, J. Christensen-Dalsgaard. *Asteroseismology*. Astronomy and Astrophysics Library. Springer Netherlands, 1 edition, 2010. ISBN 1402051786,9781402051784.

[12] B. Campbell and R. Cayrel. Spectroscopic evidence for starspots in the G dwarf HD 1835. *apjl*, 283:L17–L20, August 1984.

[13] Ostlie D.A. Carroll B.W. *An introduction to modern astrophysics*. 2ed., pearson edition, 2007. ISBN 0321442849,9780321442840.

[14] G. R. Caughlan and W. A. Fowler. Thermonuclear Reaction Rates V. *Atomic Data and Nuclear Data Tables*, 40:283, 1988.

[15] G. Cayrel de Strobel, B. Hauck, P. Francois, F. Thevenin, E. Friel, M. Mermilliod, and S. : Borde. VizieR Online Data Catalog: a Catalogue of [Fe/H] Determinations, 1991 ed. (Cayrel, 1992). *aps*, 95:273–336, October 1992.

[16] G. Cayrel de Strobel, C. Soubiran, E. D. Friel, N. Ralite, and P. Francois. A catalogue of [fe/h] determinations: 1996 edition. *A & A Supplement series*, 124 (124):299–305, 08 1997.

[17] W. J. Chaplin, Y. Elsworth, R. Howe, G. R. Isaak, C. P. McLeod, B. A. Miller, H. B. van der Raay, S. J. Wheeler, and R. New. BiSON Performance. *solphys*, 168: 1–18, September 1996.

[18] W. J. Chaplin, S. Basu, D. Huber, A. Serenelli, L. Casagrande, V. Silva Aguirre, W. H. Ball, O. L. Creevey, L. Gizon, R. Handberg, C. Karoff, R. Lutz, J. P. Marques, A. Miglio, D. Stello, M. D. Suran, D. Pricopi, T. S. Metcalfe, M. J. P. F. G. Monteiro, J. Molenda-Żakowicz, T. Appourchaux, J. Christensen-Dalsgaard, Y. Elsworth, R. A. García, G. Houdek, H. Kjeldsen, A. Bonanno, T. L. Campante, E. Corsaro, P. Gaulme, S. Hekker, S. Mathur, B. Mosser, C. Régulo, and D. Salabert. Asteroseismic Fundamental Properties of Solar-type Stars Observed by the NASA Kepler Mission. *apjs*, 210:1, January 2014.

[19] J. P. Cox and R. T. Giuli. *Principles of stellar structure* . 1968.

[20] M. P. Di Mauro. A review on Asteroseismology. *ArXiv e-prints*, March 2017.

[21] A. S. Eddington. *The Internal Constitution of the Stars*. 1926.

[22] John A. Eddy. The Maunder Minimum. *Science*, 192:1189–1202, 1976.

[23] J. W. Evans and R. Michard. Observational Study of Macroscopic Inhomogeneities in the Solar Atmosphere. I. Velocity Displacements of Fraunhofer Lines as a Function of Line Strength and Position on Disk. *apj*, 135:812, May 1962.

[24] P. Goldreich and D. A. Keeley. Solar seismology. I - The stability of the solar p-modes. *apj*, 211:934–942, February 1977.

[25] Douglas Gough. *Comments on helioseismic inference*, pages 281–318. Springer Berlin Heidelberg, Berlin, Heidelberg, 1990.

[26] D. F. Gray and S. L. Baliunas. The activity cycle of tau Ceti. *apj*, 427:1042–1047, June 1994.

[27] J. Harvey and GONG Instrument Team. The GONG Instrument Michelson Interferometer. In R. K. Ulrich, E. J. Rhodes, Jr., and W. Dappen, editors, *GONG 1994. Helio- and Astro-Seismology from the Earth and Space*, volume 76 of *Astronomical Society of the Pacific Conference Series*, page 432, 1995.

[28] A. Heger and N. Langer. Presupernova Evolution of Rotating Massive Stars. II. Evolution of the Surface Properties. *apj*, 544:1016–1035, December 2000.

[29] P. G. Judge, S. H. Saar, M. Carlsson, and T. R. Ayres. A Comparison of the Outer Atmosphere of the “Flat Activity” Star τ Ceti (G8 V) with the Sun (G2 V) and α Centauri A (G2 V). *apj*, 609:392–406, July 2004.

[30] R. Kippenhahn and H.-C. Thomas. A simple Method for the Solution of the stellar Structure Equations including Rotation and tidal Forces. *Mitteilungen der Astronomischen Gesellschaft Hamburg*, 27:168, 1969.

[31] R. B. Leighton, R. W. Noyes, and G. W. Simon. Velocity Fields in the Solar Atmosphere. I. Preliminary Report. *apj*, 135:474, March 1962.

[32] I. Lopes, D. Passos, M. Nagy, and K. Petrovay. Oscillator Models of the Solar Cycle. Towards the Development of Inversion Methods. *ssr*, 186:535–559, December 2014.

[33] A. Maeder and G. Meynet. The Evolution of Rotating Stars. *araa*, 38:143–190, 2000.

[34] E.E. Mamajek and L.A. Hillenbrand. Improved age estimation for solar-type dwarfs using activity-rotation diagnostics. *Astrophysical Journal*, 687:1264-1293, November 2008.

[35] G. Meynet and A. Maeder. Stellar evolution with rotation. I. The computational method and the inhibiting effect of the μ-gradient. *aap*, 321:465–476, May 1997.

[36] D. Naef, M. Mayor, S. G. Korzennik, D. Queloz, S. Udry, P. Nisenson, R. W. Noyes, T. M. Brown, J. L. Beuzit, C. Perrier, and J. P. Sivan. The ELODIE survey for northern extra-solar planets. II. A Jovian planet on a long-period orbit around GJ 777 A. *aap*, 410:1051–1054, November 2003.

[37] A. Satya Narayanan. *An Introduction to Waves and Oscillations in the Sun.* Astronomy and Astrophysics Library. Springer-Verlag New York, 1 edition, 2013. ISBN 978-1-4614-4399-5,978-1-4614-4400-8.

[38] F. Ochsenbein, P. Bauer, and J. Marcout. The VizieR database of astronomical catalogues. *aaps*, 143:23–32, April 2000.

[39] Y. V. Pavlenko, J. S. Jenkins, H. R. A. Jones, O. Ivanyuk, and D. J. Pinfield. Effective temperatures, rotational velocities, microturbulent velocities and abundances in the atmospheres of the Sun, HD 1835 and HD 10700. *mnras*, 422: 542–552, May 2012.

[40] B. Paxton, M. Cantiello, P. Arras, L. Bildsten, E. F. Brown, A. Dotter, C. Mankovich, M. H. Montgomery, D. Stello, F. X. Timmes, and R. Townsend. Modules for Experiments in Stellar Astrophysics (MESA): Planets, Oscillations, Rotation, and Massive Stars. *apjs*, 208:4, September 2013.

[41] E. Priest. *Magnetohydrodynamics of the Sun.* Cambridge University Press, 2014.

[42] I. Ramírez, J. Meléndez, and M. Asplund. Chemical signatures of planets: beyond solar-twins. *aap*, 561:A7, January 2014.

[43] F. J. Rogers and A. Nayfonov. Updated and Expanded OPAL Equation-of-State Tables: Implications for Helioseismology. *apj*, 576:1064–1074, September 2002.

[44] M. N. Saha. Ionisation in the Solar Chromosphere. *nat*, 105:232–233, April 1920.

[45] D. Saumon, G. Chabrier, and H. M. van Horn. An Equation of State for Low-Mass Stars and Giant Planets. *apjs*, 99:713, August 1995.

[46] D.R. Soderblom and J.R. King. Solar-type stars: Basic information on their classification and characterization. page 41, 1998.

[47] K. Stepien and E. Geyer. Rotation of solar-like main sequence stars. *aaps*, 117: 83–91, May 1996.

[48] G. Takeda, E. B. Ford, A. Sills, F. A. Rasio, D. A. Fischer, and J. A. Valenti. Structure and Evolution of Nearby Stars with Planets. II. Physical Properties of ˜1000 Cool Stars from the SPOCS Catalog. *apjs*, 168:297–318, February 2007.

[49] Y. K. Tang and N. Gai. Asteroseismic modelling of the metal-poor star τ Ceti. *aap*, 526:A35, February 2011.

[50] M. Tassoul. Asymptotic approximations for stellar nonradial pulsations. *apjs*, 43: 469–490, August 1980.

[51] T. C. Teixeira, H. Kjeldsen, T. R. Bedding, F. Bouchy, J. Christensen-Dalsgaard, M. S. Cunha, T. Dall, S. Frandsen, C. Karoff, M. J. P. F. G. Monteiro, and F. P. Pijpers. Solar-like oscillations in the G8 V star τ Ceti. *aap*, 494:237–242, January 2009.

[52] C. A. O. Torres, G. R. Quast, L. da Silva, R. de La Reza, C. H. F. Melo, and M. Sterzik. Search for associations containing young stars (SACY). I. Sample and searching method. *aap*, 460:695–708, December 2006.

[53] R. Townsend, S. Teitler, and B. Paxton. GYRE: A new open-source stellar oscillation code. In J. A. Guzik, W. J. Chaplin, G. Handler, and A. Pigulski, editors, *Precision Asteroseismology*, volume 301 of *IAU Symposium*, pages 505–506, February 2014.

[54] M. Tuomi, H. R. A. Jones, J. S. Jenkins, C. G. Tinney, R. P. Butler, S. S. Vogt, J. R. Barnes, R. A. Wittenmyer, S. O'Toole, J. Horner, J. Bailey, B. D. Carter,

D. J. Wright, G. S. Salter, and D. Pinfield. Signals embedded in the radial velocity noise. Periodic variations in the τ Ceti velocities. *aap*, 551:A79, March 2013.

[55] F. van Leeuwen. Validation of the new Hipparcos reduction. *aap*, 474:653–664, November 2007.

[56] M. Wenger, F. Ochsenbein, D. Egret, P. Dubois, F. Bonnarel, S. Borde, F. Genova, G. Jasniewicz, S. Laloë, S. Lesteven, and R. Monier. The SIMBAD astronomical database. The CDS reference database for astronomical objects. *aaps*, 143:9–22, April 2000.

This page was left Blank

Appendix A

TABLE 2

CLASSIFICATION OF VARIABILITY IN PROGRAM STARS

HD Number	Star	Figure 1 Reference	$B-V$	Spectral Type[a]	$\langle S \rangle$[m]	Primary Classification[n]: $P_{cyc} \pm \Delta P$ (yr)	Primary Classification[n]: FAP Grade	Secondary Classification[o]
...	Sun	1*d*	0.66	G2 V	0.179	10.0 ± 0.1	Excellent	...
1835	9 Cet	1*d*	0.66	G2 V	0.349	9.1[p] ± 0.3	Fair	Long
2454		1*a*	0.43	F2 V	0.170	Var	...	...
3229	14 Cet	1*a*	0.44	F2 V[b]	0.224	4.9 ± 0.1	Poor	...
3443		1*e*	0.72	G5 V	0.183	Var	...	Long
3651	54 Psc	1*f*	0.85	K0 V	0.176	13.8 ± 0.4[p,q]	Good	Long
3795		1*e*	0.70	G3 V	0.156	Var	...	...
4628		1*g*	0.88	K4 V	0.230	8.37 ± 0.08	Excellent	...
6920	44 And	1*c*	0.60	F8 V	0.194	Var	...	...
9562		1*d*	0.64	G2 V[b]	0.136	Long	...	...
10476	107 Psc	1*f*	0.84	K1 V	0.198	9.6 ± 0.1	Excellent	...
10700	τ Cet	1*e*	0.72	G8 Vp	0.171	Flat ?[r]	...	...
10780		1*f*	0.81	K0 V[c]	0.280	>7[s]	...	...
12235	112 Psc	1*d*	0.62	G1 V[b]	0.160	Var	...	...
13421	64 Cet	1*c*	0.56	F8 V[b]	0.131	Flat	...	...
16160		1*g*	0.98	K3 V	0.226	13.2 ± 0.2	Excellent	...
16673		1*b*	0.52	F8 V	0.215	Var	...	...
17925		1*f*	0.87	K0 V	0.653	Long	...	...
18256	ρ^3 Ari	1*a*	0.43	F5 V	0.185	6.8 ± 0.2	Fair	...
20630	κ Cet	1*e*	0.68	G5 V	0.366	5.6[p] ± 0.1	Fair	Long
22049	ϵ Eri	1*g*	0.88	K2 V	0.496	Var	...	Long
22072		1*g*	0.89	G7 V[b]	0.131	Var	...	...
23249	δ Eri	1*g*	0.92	K0 IV[d]	0.137	Flat?	...	...
25998	50 Per	1*a*	0.46	F7 V	0.300	Long	...	...
26913	V891 Tau	1*e*	0.70	G8 V[e]	0.396	7.8[p] ± 0.2	Fair	Long
26923	V774 Tau	1*c*	0.59	G0 V[b,e]	0.287	Var	...	...
26965	o^2 Eri	1*f*	0.82	K1 V	0.206	10.1 ± 0.1	Excellent	...
29645		1*c*	0.57	G3 V	0.140	Long	...	...
30495	58 Eri	1*d*	0.63	G1 V	0.297	Var	...	...
32147		1*g*	1.06	K5 V	0.286	11.1 ± 0.2	Excellent	Long
33608		1*a*	0.46	F6 V	0.214	Long	...	...
35296	111 Tau	1*b*	0.53	F8 V	0.332	Long	...	...
37394		1*f*	0.84	K1 V	0.453	3.6[s] ± 0.1	Poor	...
39587	χ^1 Ori	1*c*	0.59	G0 V	0.325	Var	...	Long
43587		1*d*	0.61	G0 V	0.156	Flat?	...	...
45067		1*c*	0.56	F8 V	0.141	Flat	...	...
61421	α CMi	1*a*	0.42	F5 IV–V	0.171	Var	...	...
72905	π^1 UMa	1*d*	0.62	F7 V	0.367	Var	...	...
75332		1*b*	0.49	F7 V	0.279	Var	...	...
76151		1*d*	0.67	G3 V	0.246	2.52[p] ± 0.02	Fair	Long
76572	61 Cnc	1*a*	0.43	F3 V	0.148	7.1 ± 0.2	Poor	...
78366		1*c*	0.60	G0 V	0.248	12.2 ± 0.4	Good	5.9 ± 0.1, fair
81809		1*d*	0.64	G2 V	0.172	8.17 ± 0.08	Excellent	...
82443		1*f*	0.77	K0 V[f]	0.635	2.8[s] ± 0.1	Poor	...
82885	11 LMi	1*e*	0.77	G8 IV–V[d]	0.284	7.9 ± 0.2	Fair	12.6 ± 0.7, poor
88355	34 Leo	1*a*	0.46	F6 V	0.170	Var	...	...
88737		1*b*	0.56	F5 V[g]	0.234	24?	...	...
89744		1*b*	0.54	F6 V	0.137	Flat	...	...
95735	Lld 21185	1*g*	1.51	M2.1 Ve[h]	0.424	Var	...	...
97344		1*d*	0.61	G0 V	0.335	Var	...	...
100180	88 Leo	1*c*	0.57	F7 V	0.165	3.56 ± 0.04	Fair	12.9 ± 0.5, fair
100563	89 Leo	1*a*	0.46	F5 V	0.202	Var	...	...
101501	61 UMa	1*e*	0.72	G8 V	0.311	Var	...	Long
103095	Gmb 1830	1*e*	0.75	G8 VI	0.188	7.30 ± 0.08	Excellent	...
106516		1*a*	0.46	F6 V	0.208	Var	...	...
107213	9 Com	1*b*	0.50	F8 V	0.135	Long	...	...
111456		1*a*	0.46	F6 V	0.300	7[s]?	...	...
114378	α Com	1*a*	0.45	F5 V + F5 V	0.244	Long	...	...
114710	β Com	1*c*	0.57	G0 V	0.201	16.6 ± 0.6	Good	9.6 ± 0.3, fair
115043		1*c*	0.60	G1 V[f]	0.327	Var	...	...
115383	59 Vir	1*c*	0.58	F8 V	0.313	Var	...	...
115404		1*g*	0.93	K1 V[f]	0.535	12.4 ± 0.4	Good	...
115617	61 Vir	1*e*	0.71	G6 V	0.162	Var	...	...
120136	τ Boo	1*b*	0.48	F7 V[b]	0.191	11.6 ± 0.5	Poor	...
124570	14 Boo	1*b*	0.54	F6 V[b]	0.133	Flat	...	...
124850	ι Vir	1*b*	0.52	F7 IV[i]	0.210	Long	...	...
126053		1*d*	0.63	G3 V	0.165	22?	...	...
129333	EK Dra	1*d*	0.61	G0 V[j]	0.544	Var	...	...

TABLE 2—*Continued*

HD Number	Star	Figure 1 Reference	$B-V$	Spectral Type[a]	$\langle S \rangle$[m]	Primary Classification[n]		Secondary Classification[o]
						$P_{cyc} \pm \Delta P$ (yr)	FAP Grade	
131156A	ξ Boo A	1*e*	0.76	G8 V	0.461	Var	...	...
131156B........	ξ Boo B	1*g*	1.17	K4 V	1.381	Long	...	...
136202	5 Ser	1*b*	0.54	F8 IV–V[k]	0.140	Long	...	...
137107AB......	η CrB	1*c*	0.58	G2 V + G2 V	0.184	Var	...	...
141004	λ Ser	1*d*	0.60	G0 V	0.155	Long	...	...
142373	χ Her	1*c*	0.56	F9 V	0.147	Flat	...	...
143761	ρ CrB	1*d*	0.60	G2 V	0.150	Long	...	...
149661	12 Oph	1*f*	0.82	K0 V	0.339	17.4 ± 0.7	Good	4.00 ± 0.04, Good
152391		1*e*	0.76	G7 V[f]	0.393	10.9 ± 0.2	Excellent	...
154417		1*c*	0.57	F8 V[b]	0.269	7.4 ± 0.2	Fair	...
155885	36 Oph B	1*f*	0.86	K1 V	0.384	5.7 ± 0.1	Poor	...
155886	36 Oph A	1*f*	0.86	K0 V	0.375	Var	...	Long
156026		1*g*	1.16	K5 V[f]	0.770	21.0 ± 0.9	Good	...
157856		1*a*	0.46	F5 V[g]	0.202	15.9 ± 0.8	Fair	...
158614		1*e*	0.72	G8 IV–V	0.158	Flat	...	...
159332		1*b*	0.48	F4 V	0.144	Flat?	...	...
160346		1*g*	0.96	K3 V[f]	0.300	7.00 ± 0.08	Excellent	...
161239	84 Her	1*d*	0.65	G6 V[l]	0.138	5.7 ± 0.1	Fair	11.8 ± 0.5, poor
165341A	70 Oph A	1*f*	0.86	K0 V	0.392	5.1 ± 0.1	Fair	...
165341B........	70 Oph B	1*g*	1.16	K6 V	0.691	Var	...	...
166620		1*f*	0.87	K2 V	0.190	15.8 ± 0.3	Excellent	...
176051		1*c*	0.59	G0 V	0.176	10[q]?	...	...
176095		1*a*	0.46	F5 IV[j]	0.202	Long	...	...
178428		1*e*	0.70	G4 V	0.154	Flat	...	...
182101		1*a*	0.44	F6 V	0.216	5.1 ± 0.1	Poor	...
182572	31 Aql	1*f*	0.77	G8 IV	0.148	Flat	...	...
185144	σ Dra	1*f*	0.80	K0 V	0.215	7[r]?	...	...
187013	17 Cyg	1*b*	0.47	F5 V	0.154	Long	...	...
187691	*o* Aql	1*b*	0.55	F8 V	0.148	5.4 ± 0.1	Fair	...
188512	β Aql	1*f*	0.86	G8 IV[d]	0.136	4.1[s] ± 0.1	Poor	...
190007		1*g*	1.17	K4 V[j]	0.746	13.7 ± 0.7	Fair	5.3 ± 0.1, poor
190360		1*e*	0.73	G6 IV[d]	0.146	Flat	...	...
190406	15 Sge	1*d*	0.61	G1 V	0.194	2.60 ± 0.02	Fair	16.9 ± 0.8, good
194012		1*b*	0.51	F5 V[j]	0.198	16.7 ± 0.9	Poor	5.4 ± 0.1, fair
201091	61 Cyg	1*g*	1.18	K5 V	0.658	7.3 ± 0.1	Excellent	...
201092		1*g*	1.37	K7 V	0.986	11.7 ± 0.4	Good	...
206860	HN Peg	1*c*	0.59	G0 V	0.330	6.2 ± 0.2	Poor	...
207978	15 Peg	1*a*	0.42	F0 V[b]	0.152	Flat	...	...
212754	34 Peg	1*b*	0.52	F5 V	0.140	Long	...	...
216385	σ Peg	1*b*	0.48	F7 IV	0.142	Flat	...	...
217014	51 Peg	1*e*	0.67	G5 V[b]	0.149	Var	...	...
219834A	94 Aqr A	1*f*	0.80	G5 IV–V	0.155	21 ± 1	Good	...
219834B........	94 Aqr B	1*g*	0.91	K2 V	0.204	10.0 ± 0.2	Excellent	...
224930	85 Peg	1*e*	0.67	G3 V	0.184	10.2[p] ± 0.4	Poor	Long

NOTE.—Variability classification: "Var" means significant variability without pronounced periodicity, on timescales longer than 1 yr but much shorter than 25 yr ($\langle \sigma_S/S \rangle \gtrsim 2\%$). "Flat" means $\langle \sigma_S/S \rangle < 1\%–1.5\%$. "Flat?" means $\langle \sigma_S/S \rangle \approx 1.5\%–2\%$. "Long" means significant variability on timescales longer than 25 yr. Note that some records show secular change over 25 yr which suggests that, if present, cycle period > 50 yr.

[a] Spectral type except for Sun from Third Edition of the Catalogue of Bright Stars (Hoffleit 1964) unless otherwise noted. Spectral type and $B-V$ for the Sun from Keenan 1991 and Hardorp 1980, respectively.

[b] Spectral type from Fifth Edition of the Catalogue of Bright Stars (Hoffleit & Warren 1991) indicates that luminosity class may be IV or IV–V.

[c] Listed erroneously in Fifth Edition as M1 III.

[d] Absolute magnitude determined from the width of the Ca II lines (Wilson 1976) confirm that star is above the main sequence.

[e] Soderblom & Mayor 1993 list the spectral types for HD 26913 and HD 26923 as G8 V and G0 V, respectively, as observed by Slettebak 1963. Stephenson 1960 observed them as G5 IV + G0 IV, but Wilson & Skumanich 1964 observations of Sr II λ4077 place them firmly on the main sequence.

[f] Spectral type from A Supplement to the Bright Star Catalogue (Hoffleit, Saladyga, & Wlasuk 1983).

[g] Buscombe 1980.

[h] Buscombe 1984.

[i] Wilson 1984 finds no Ca II emission, and Sr II λ4077 comparable in strength to Fe I λ4063. Doubtful that it is F6 III as listed in Fifth Edition.

[j] Buscombe 1977.

[k] Listed in Fifth Edition as F8 III–IV; 10 Å mm^{-1} spectra preclude it being III.

[l] On 10 Å mm^{-1} spectrograms obtained by Wilson prior to the beginning of the survey, the intensity of Sr II λ4077 is much weaker than that of Fe I λ4063 (Wilson 1984). Thus, the star is less luminous than class III as listed in both the Fourth and Fifth Editions of the Catalogue of Bright Stars.

[m] Annually averaged mean over all years.

[n] If cyclic, period P_{cyc}, $\pm\Delta P$, and FAP (in percent) grade are listed as excellent $\equiv FAP \leq 10^{-9}$, good $\equiv 10^{-9} < FAP \leq 10^{-5}$, fair $\equiv 10^{-5} < FAP \leq 10^{-2}$, and poor $\equiv 10^{-2} < FAP \leq 10^{-1}$.

[o] Secondary period present in the periodogram after the primary frequency was filtered out, or behavior on timescales > 25 yr.

[p] Linear trend removed prior to period identification.

[q] Maunder-minimum activity beginning after 1980?

[r] Possible increasing activity after 1988.

[s] Sparse data prior to 1980, not included in periodogram analysis.